348 *J. Am. Chem. Soc.* **1994**, *116*, 348-361

Polysiloxane-Bound Ether–Phosphines and Ruthenium Complexes. A Characterization by Solid-State NMR Spectroscopy and Catalysis[1]

Ekkehard Lindner,* Martin Kemmler, Hermann A. Mayer, and Peter Wegner

Contribution from the Institut für Anorganische Chemie der Universität, Auf der Morgenstelle 18, D-72076 Tübingen, Germany

Received May 19, 1993[⊗]

Abstract: The monomeric ether–phosphine ligands $(CH_3O)_3Si(CH_2)_3(Ph)PCH_2D$ [D = CH_2OCH_3 (**1a**), tetrahydrofuryl (**1b**), and 1,4-dioxanyl (**1c**)] and their P-coordinated trimethoxysilyl- (T-) functionalized ruthenium(II) complexes $HRuCl(CO)(P{\sim}O)_3$ (**3a–c**) were copolymerized with variable amounts of $Si(OEt)_4$ (Q elements) under various sol–gel conditions to give the polysiloxane-bound ether–phosphine ligands **1a′(Q^n)$_x$–1c′(Q^n)$_x$** and (ether–phosphine)ruthenium(II) complexes **3a′(Q^n)$_x$–3c′(Q^n)$_x$**, [P∼O: η^1-P-coordinated; **(Q^n)$_x$**: x = number of cocondensated Q type silicon atoms, n = 2–4, the number of Si–O–Si bonds]. Detailed ^{31}P and ^{13}C spin–lattice relaxation time studies (T_{1P}, T_{1C}, $T_{1\rho H}$) show that the noncomplexed ether–phosphine ligands strongly increase their mobilities in the gels at rising temperatures, while the coordinated ligands in the complexes are less mobile and rigidly bound to ruthenium. Solid-state ^{29}Si NMR spectroscopy has been used to determine the relative amounts of the T and Q silyl species and the degree of condensation. Moreover, the molecular mixing of the copolymerized components in the samples has been investigated and the transition to the silica gel attached system **3c′–silica gel** elucidated. The materials, obtained by the different sol–gel variants, differ in their amount of Q species, degree of condensation, and their particle sizes, which strongly influence their catalytic behavior. Although the BET surfaces are in the range of the external surface of the gels, a high catalytic activity has been found when small particle sizes have been combined with a low content of Q silicon moieties. This can be traced back to a high flexibility of such materials, which allows swelling and an increase of the surface during hydrogenation of *n*-butyraldehyde to butanol within the gel. The undesired tendency to form highly swollen gels in alcohols after catalysis, which complicate the separation of the catalysts from the products, has been suppressed without loss of catalytic activity by the use of a modified matrix containing small amounts of insoluble ionic magnesium silicates. Constant elemental analyses of this material after three identical catalytic runs demonstrate the possibilities of this system, which unifies the advantages of organic and inorganic polymer networks and those of homogeneous and heterogeneous catalyses.

Introduction

Over the past few years considerable progress has been made in the preparation and application of immobilized reagents.[2] Inorganic oxides as base matrices, especially synthetic silicates, have gained outstanding importance due to their diversity in physical properties, their purity and chemical resistance, and the ease of functionalization through silanol groups.[3] In contrast to *surface*-modified inorganic materials,[4–6] simultaneous cocondensation of organo-functionalized silanes $R{-}Si(OMe)_3$ with $Si(OEt)_4$ (sol–gel process[7]) yields novel networks with preferable mechanical and chemical properties, namely, a high degree of flexibility and ligand densities as well as a reduced leaching of functional groups:[8,9]

$$x\mathrm{R{-}Si(OMe)_3} + y\mathrm{Si(OEt)_4} + ((3x + 4y)/2)\mathrm{H_2O} \rightarrow \underset{\text{T groups}}{[\mathrm{R{-}SiO_{3/2}}]_x}\underset{\text{Q groups}}{[\mathrm{SiO_{4/2}}]_y} + 3x\mathrm{MeOH} + 4y\mathrm{EtOH} \qquad (1)$$

When R contains donor atoms (such as P, O, N, or S), trimethoxysilyl- (T-) functionalized organometallic complexes can be synthesized and copolymerized to three-dimensional networks.[1,8–11] Our approach to achieve this goal was to generate T-functionalized ligands containing oxygen and phosphorus as donor atoms. This type of a potentially bidentate ligand has recently found application in coordination chemistry and homogeneous catalysis.[12] A flexible α,ω-alkanediyl spacer was used to link the ether–phosphine moiety to the support. These versatile building blocks allow us to tailor and tune the properties of the materials to various applications.

Heteronuclear cross-polarization magic-angle spinning (CP-MAS) solid-state NMR spectroscopy has been shown to be a powerful tool for investigating insoluble and noncrystalline solids.[3,13,14] The phosphorus nucleus has been a most suitable

---

[⊗] Abstract published in *Advance ACS Abstracts*, December 1, 1993.

(1) Supported Organometallic Complexes. 5. Part 4: Lindner, E.; Schreiber, R.; Kemmler, M.; Mayer, H. A.; Fawzi, R.; Steimann, M. *Z. Anorg. Allg. Chem.* **1993**, *619*, 202–208.

(2) Deschler, U.; Kleinschmit, P.; Panster, P. *Angew. Chem.* **1986**, *98*, 237–253; *Angew. Chem., Int. Ed. Engl.* **1986**, *25*, 236.

(3) Eckert, H. *Prog. Nucl. Magn. Reson. Spectrosc.* **1992**, *24*, 159–293.

(4) Maciel, G. E.; Sindorf, D. W.; Bartuska, V. *J. Chromatogr.* **1981**, *205*, 438–443.

(5) Sindorf, D. W.; Maciel, G. E. *J. Am. Chem. Soc.* **1983**, *105*, 3767–3776.

(6) Bayer, E.; Albert, K.; Reiners, J.; Nieder, M.; Müller, D. *J. Chromatogr.* **1983**, *264*, 197–213.

(7) Khatib, I. S.; Parish, R. V. *J. Organomet. Chem.* **1989**, *369*, 9–16.

(8) Lindner, E.; Bader, A.; Mayer, H. A. *Z. Anorg. Allg. Chem.* **1991**, *598/599*, 235–252.

(9) Lindner, E.; Bader, A.; Mayer, H. A. *Inorg. Chem.* **1991**, *30*, 3783–3785.

(10) (a) Lindner, E.; Kemmler, M.; Mayer, H. A. *Chem. Ber.* **1992**, *125*, 2385–2390. (b) Lindner, E.; Kemmler, M.; Mayer, H. A. *Z. Anorg. Allg. Chem.*, in press.

(11) Schubert, U.; Egger, C.; Rose, K.; Alt, C. *J. Mol. Catal.* **1989**, *55*, 330–339.

(12) Bader, A.; Lindner, E. *Coord. Chem. Rev.* **1991**, *108*, 27–110 and references cited therein.

(13) Fyfe, C. A. *Solid State NMR for Chemists*; CRC Press: Guelph, ON, 1984.

(14) Fyfe, C. A.; Zhang, Y.; Aroca, P. *J. Am. Chem. Soc.* **1992**, *114*, 3252–3255.

0002-7863/94/1516-0348$04.50/0

probe to investigate supported phosphines and the stereochemistry of immobilized complexes.[8-10,15-17] Carbon-13 CP-MAS NMR spectroscopy has been used to verify the integrity of the ligand framework.[1,10,15,16] In addition, solid-state ^{29}Si NMR spectroscopy is a unique method for characterizing the support of sol-gel materials.[1,8-10,14,18] Moreover, scanning microscopy (AFM, SEM) combined with the BET method has been used to characterize the surfaces of sol-gel products.[18]

Although a lot of synthetic work has been undertaken, there is still a lack of detailed structural information about such materials. In this study, we characterize sol-gel matrices of materials polymerized under various conditions and with a range of complex densities. Furthermore, the dynamic behaviors of different polysiloxane-bound ether-phosphine ligands and their ruthenium complexes are described. In addition, we correlate sol-gel routes, cross-linking, particle sizes, and surface areas with catalytic activities in hydrogenation experiments.

Results and Discussion

Preparation of the Monomeric Complexes 3a-c. In the case of trimethoxysilyl- (T-) modified phosphines such as **1a-c**, the generally applied synthesis of complexes of the type HRuCl(CO)(PR$_3$)$_3$ from RuCl$_3$ and an excess of the phosphine and aqueous formaldehyde in alcohols[19] is not applicable. This is due to hydrolysis of the T-functionality, undesirable at this stage, and a possible redox reaction between RuCl$_3$ and the phosphines. Therefore, the phosphines in HRuCl(CO)(PPh$_3$)$_3$ (**2**) were exchanged with the more basic ether-phosphines **1a-c** by treating **2** with **1a-c** in toluene (Scheme 1). This reaction was found to be a very fast, simple, and quantitative method for the preparation of the T-functionalized ruthenium complexes HRuCl(CO)(P~O)$_3$ (**3a-c**). The solid-state ^{29}Si NMR spectra of **3a-c** show a sharp signal at -42.3 ppm due to the unhydrolyzed T^0 function, -(CH$_2$)$_3$Si(OMe)$_3$.

Sol-Gel Processing. In previous studies, T-functionalized ether-phosphine complexes of ruthenium(II) and palladium(II) have been polycondensated in the absence of Si(OEt)$_4$.[1,10] These polymers show a low degree of condensation[20] (59-77%) and consist of branched polyorganosiloxane chains, which are connected via ruthenium and palladium complexes to form relatively open three-dimensional networks. The retention of the stereochemistry of the transition metal complexes and the Si-C bond during the gelation process has been established by ^{31}P, ^{13}C, and ^{29}Si solid-state NMR spectroscopy.[1,10] However, for many applications, e.g., catalysis or chromatography, it is favorable to design two- or three-dimensional polysiloxane matrices in a cross-linking copolymerization of Si(OEt)$_4$ with T-functions.[7-9,11] In this process, it is expected that the T species are concurrently incorporated together with Q species or that the matrix, which is formed, contains domains of either T or Q groups. The sol-gel process can be described by the reaction scheme given in Scheme 2.[3] Suitable monomer precursors are first hydrolyzed, and the resulting colloidal solutions subsequently undergo polymerization. The hydrated, highly swollen gels are then dried to obtain further condensation and densification.

When organometallic complexes, such as **3a-c**, are incorporated by sol-gel processing, they have to be chemically inert toward their T-functionalized phosphines, water, Si(OEt)$_4$, and the polycondensation catalyst. Thus, the sol-gel process has to be adjusted to individual properties of the complexes. Several pathways of sol-gel processing have been applied which can be considered as examples of various possibilities of creating functionalized polysiloxane materials.

In method 1 (see the Experimental Section), the components were homogenized with a minimum amount of methanol and a catalytic amount of (n-Bu)$_2$Sn(OAc)$_2$. Hydrolysis and condensation steps increased slowly the viscosity of the warmed mixture, and eventually solidification led to a highly swollen gel. When the supporting solvent was removed in vacuo, the cavities in the polymer network collapsed with a multiple loss of its volume. Since the resulting gel did not undergo swelling in alcohols to its original volume, it is implied that simultaneous condensation of

Scheme 1

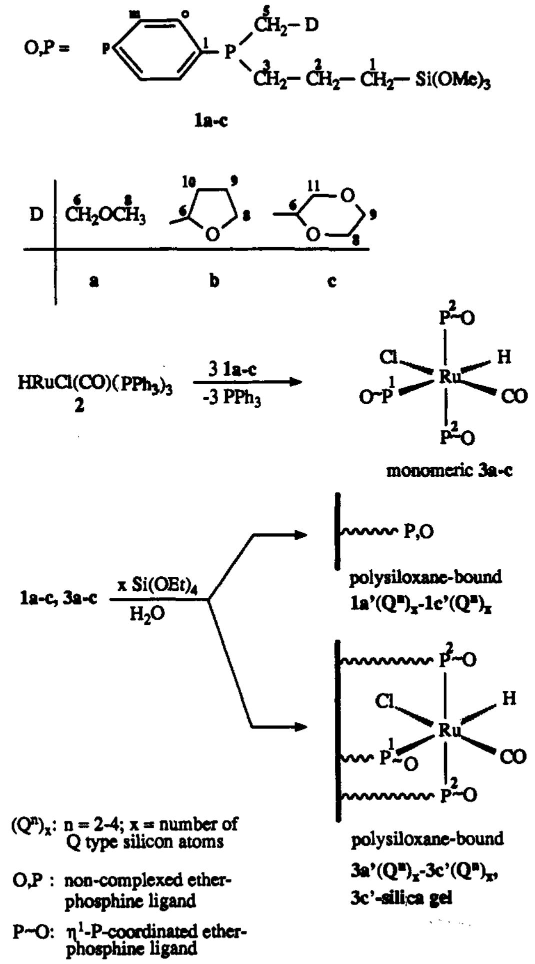

Scheme 2

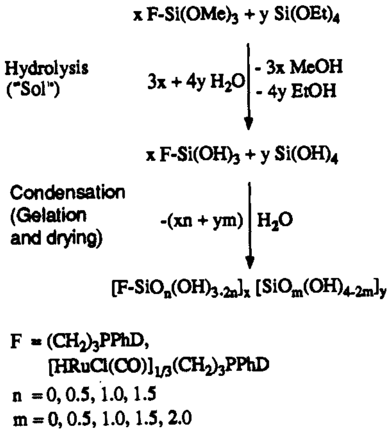

---

[15] Liu, D. K.; Wrighton, M. S.; McKay, D. R.; Maciel, G. E. *Inorg. Chem.* **1984**, *23*, 212-220.

[16] Komoroski, R. A.; Magistro, A. J.; Nicholas, P. P. *Inorg. Chem.* **1986**, *25*, 3917-3925.

[17] Bemi, L.; Clark, H. C.; Davies, J. A.; Fyfe, C. A.; Wasylishen, R. E. *J. Am. Chem. Soc.* **1982**, *104*, 438-445.

[18] Shea, K. J.; Loy, D. A.; Webster, O. *J. Am. Chem. Soc.* **1992**, *114*, 6700-6710.

[19] Ahmad, N.; Levison, J. J.; Robinson, S. D.; Uttley, M. F. *Inorg. Synth.* **1974**, *15*, 48.

[20] Degree of condensation of the T species = $100(T^1 + 2T^2 + 3T^3)/[3(T^1 + T^2 + T^3)]$, degree of condensation of the Q species = $100(2Q^2 + 3Q^3 + 4Q^4)/[4(Q^2 + Q^3 + Q^4)]$; T^1, T^2, T^3, Q^2, Q^3, and Q^4 are the relative amounts of silyl species present in the sample (Table 3).

silanol groups occurred. The hardened, brittle gels were ground mechanically into fine powders. Subsequent separation of free PPh_3 was practicable by stirring the powdered material in *n*-hexane ("solvent processing").

The precipitation of the hydrolyzed complexes **3a–c** and $Si(OEt)_4$ was carried out by method 2a (see the Experimental Section). At low concentrations of the components in methanol [0.2 M solution of $Si(OEt)_4$], no gel transition was observed. After the addition of aqueous NH_4HCO_3, coagulation and condensation occurred, leading to fine, cloudy precipitates. The gel was isolated and stirred with dry acetone to facilitate condensation steps and to remove physically adsorbed water. In contrast to method 1, further drying in vacuo generated ultrafine gel particles.

In method 2b, an excess of dry $MgSO_4$ was added to the hydrolyzed complexes instead of aqueous NH_4HCO_3 to remove the water and to initiate the condensation and the gel transition.

In method 3, silica gel was prepared from $Si(OEt)_4$ alone and subjected to a second sol–gel reaction with the monomer **3c** to give the immobilized complex **3c′–silica gel**.

The different materials obtained by the above procedures (methods 1–3) were characterized by heteronuclear solid-state NMR spectroscopy, scanning electron microscopy, and surface area determinations. With this knowledge the catalytic behaviors of the polysiloxane-bound ruthenium complexes in hydrogenation of butyraldehyde will be described.

Characterization by Solid-State NMR. One-dimensional heteronuclear solid-state NMR spectroscopy can be used to yield a great variety of complementary information. Cross polarization constants T_{XH}, which can be calculated from the variation of the contact time, and spin–lattice relaxation times T_{1X} (X = Si, C, or P) are typical of different Si, C, and P nuclei in the materials.[21] Thus, local environments of the nuclei can be observed. The relaxation time of the protons in the rotating frame, $T_{1\rho H}$, however, is not specific to the various nuclei, but rather, it is a quantity which is averaged within domains of 1–2 nm in diameter, at least in those cases where there is sufficient dipolar coupling among the protons to provide spin diffusion.[21-23] If these dynamic aspects are taken into account, valuable quantitative information can be obtained. Thus, in the case of quantitative ^{29}Si CP-MAS NMR spectroscopy, the correct proportion of the silyl species, T:Q, the degree of condensation,[20] and the distribution of the T-functionalities throughout the polysiloxane matrix can be described.

^{29}Si Solid-State NMR Spectroscopy. In Figure 1, ^{29}Si CP-MAS NMR spectra of the polysiloxane-bound complex HRuCl(CO)(P∼O)$_3$, **3b′(Q^0)$_6$**, obtained at two different contact times T_C, are depicted. This complex has been prepared according to method 1 by cocondensation with six equiv of $Si(OEt)_4$ (T:Q = 1:2, Schemes 1 and 2). The silyl species in Figure 1 and the corresponding ^{29}Si chemical shifts[5,6,24] are summarized in Table 1. As evident from Figure 1, various contact times T_C result in different peak intensities in the ^{29}Si CP-MAS NMR spectra. Due to the strong dependence of the cross polarization efficiency on the internuclear distances between protons and the various silicon atoms, the relative peak intensities cannot be used to portray the correct population in the sample.[21,25,26] However, the observed signal intensities $I(T_C)$ can be corrected by performing variable contact time studies under conditions of the Hartmann–Hahn match. The amplitude $I(T_C)$ of each signal observed in the ^{29}Si spectrum at the contact time T_C has been described by the following "classical" equation:[26]

$$I(T_C) = I_0/\left(1 - \frac{T_{SiH}}{T_{1\rho H}}\right)(e^{-T_C/T_{1\rho H}} - e^{-T_C/T_{SiH}}) \qquad (2)$$

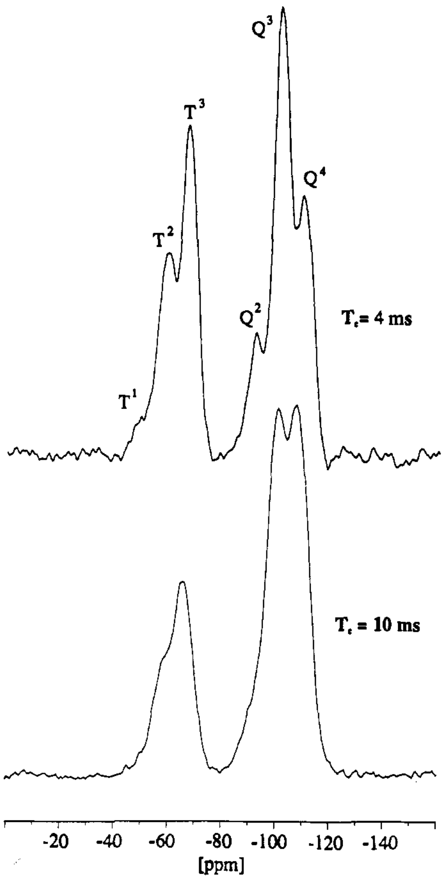

Figure 1. Solid-state ^{29}Si CP-MAS NMR spectra of **3b′(Q^0)$_6$** prepared by method 1 at different contact times T_C.

The value of I_0 represents the relative amount of each of the silyl species present in the sample.

First of all, cross polarization constants T_{SiH} (see Table 1) were determined by a fit of eq 2 to the intensities of the signals $I(T_C)$ as a function of the contact time T_C. Silicon atoms with an equal number of proton-containing substituents have similar T_{SiH} constants (T^2/Q^2 and T^3/Q^3). The fully condensed Q^4 species with rather long ^{29}Si–^{1}H distances magnetize the slowest. The T_{SiH} constants for the Q species of the polysiloxane-bound complexes (see Table 1 and the Experimental Section) are in the range of those determined for silica gel prepared by method 3: 1.07 ms (Q^2), 1.86 ms (Q^3), and 3.90 ms (Q^4). It is evident that the T_{SiH} constants, especially those of the silyl species in the T/Q copolymers, must be considered as an average value of all possible local environments of the particular silicon species.

Secondly, the loss of proton magnetization in the rotating frame, described by $T_{1\rho H}$,[27] has to be investigated to obtain the quantitative ratios I_0 of the various T and Q species (eq 2) and to describe the distribution of the T-anchored ruthenium complexes throughout the material.

As shown in Figure 2A by the sample **3b′(Q^0)$_6$**, $T_{1\rho H}$ is constant (5.4 ± 0.2 ms) for all protons near the T and Q silicon atoms with no dependence on the applied contact time T_C (4 and 10 ms) having been observed. Obviously, $T_{1\rho H}$ is a uniform quantity in the sample due to efficient dipolar coupling of the protons. This indicates, that the ligand-containing T species and the Q groups

---

[21] Voelkel, R. *Angew. Chem.* **1988**, *100*, 1525–1540; *Angew. Chem., Int. Ed. Engl.* **1988**, *27*, 1468.

[22] Koenig, J. L.; Andreis, M. *Solid State NMR of Polymers*; Mathias, L. J., Ed.; Plenum Press: New York, 1991; pp 201–213.

[23] Komoroski, R. A. *High Resolution NMR Spectroscopy of Synthetic Polymers in Bulk*; VCH Publishers, Inc.: Deerfield Beach, FL, 1986; pp 63–226, 247–306.

[24] Pfleiderer, B.; Albert, K.; Bayer, E.; van den Ven, L.; de Haan, J.; Cramers, C. *J. Phys. Chem.* **1990**, *94*, 4189–4194.

[25] Harris, R. K. *Analyst* **1985**, *110*, 649–655.

[26] Mehring, M. In *Principles of High Resolution NMR in Solids*, 2nd ed.; Springer-Verlag: Berlin, Heidelberg, New York, 1983; pp 143–155.

[27] Schaefer, J.; Stejskal, E. O.; Buchdahl, R. *Macromolecules* **1977**, *10*, 384–405.

Table 1. Silyl Species, δ ^{29}Si, T_{SiH}, and Relative [$I(T_c)$] and Corrected Relative Values I_0 of the Silyl Moieties in **3b′(Q■)₆**

notation	structural type	δ ^{29}Si (ppm)	T_{SiH} (ms)	I_0 [I(4 ms)]	I_0 [I(5 ms)]	I_0 [I(8 ms)]	I_0 [I(10 ms)]	MAS(SPE)
T^1	$O_{1/2}Si(OH)_2F^a$	–49.9		0.8 (0.8)	0.5 (0.5)	0.4 (0.3)	0.5 (0.4)	0.6
T^2	$O_{2/2}Si(OH)F$	–59.2	1.45	3.1 (3.2)	3.4 (3.4)	2.8 (2.7)	3.0 (2.8)	3.0
T^3	$O_{3/2}SiF$	–66.5	1.95	6.1 (6.0)	6.2 (6.1)	6.8 (7.0)	6.5 (6.8)	6.4
Q^2	$O_{2/2}Si(OH)_2$	–91.6	1.46	2.1 (2.2)	1.8 (1.7)	2.0 (1.9)	2.2 (2.1)	2.2
Q^3	$O_{3/2}Si(OH)$	–100.5	2.04	*b*	*b*	9.6 (10.0)	9.1 (9.6)	9.2
Q^4	$O_{4/2}Si$	–108.6	3.43	*b*	*b*	9.1 (10.1)	8.2 (10.2)	8.4

[a] F = $(CH_2)_3PPhD(HRuClCO)_{1/3}$. [b] Contact time is too short for cross polarization of Q^3 and Q^4 species.

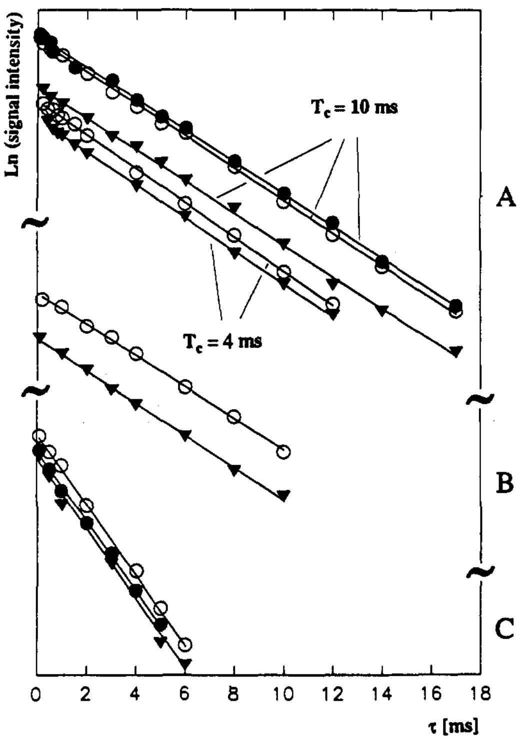

Figure 2. $T_{1\rho H}$ via ^{29}Si: A, **3b′(Q■)₆**; B, **3a′(Q■)₆**; C, **1a′(Q■)₂** (▼, T^3; ○, Q^3; ●, Q^4).

are covalently bound and mixed in the gel. Hence, the ruthenium complexes, which are fixed by the T groups via the ether–phosphine ligand, are distributed homogeneously across the whole T/Q copolymer. Surprisingly low, single exponential $T_{1\rho H}$ values for the protons of the T and Q silicon species have been found for the ether–phosphine ligands **1a′(Q■)₂–1c′(Q■)₂** and **1c′(Q■)₁₀** (Table 2 and Figure 2C).

Upon coordination of three immobilized phosphine ligands to one ruthenium to form the complexes **3a′(Q■)ₓ–3c′(Q■)ₓ** (x = 3.4–10), $T_{1\rho H}$ increases to a typical value of 5.4–5.5 ms (Table 2 and Figure 2A,B). The fact that all protons in the polysiloxane matrix, even those of the Q species, change their $T_{1\rho H}$ quantity *equally* upon complexation clearly demonstrates that the T functions of the ruthenium complexes are thoroughly mixed with the Q moieties. In the case of domain structures, which may be formed from either T or Q species, Q^4 silicon atoms located too far from protons (typically four bonds) would not contribute significantly to the intensity of the Q^4 signal in the spectrum. Such "problematic" Q^4 silicons are present in silica gels and silicon glasses in a considerable amount.[3,28,29] Therefore, the number of nondetectable "bulk" species depends on the ratio of T:Q. At low Q contents (x = 3.4–10, see above) and if the T and Q silicons are totally disordered in the polysiloxane matrix, the total amount of Q^4 species has to contribute to the intensity of the signal according to eq 2. However, for a quantitative determination, the condition $T_{1\rho H} \gg T_{SiH}$ must be satisfied.[25] The Q^4 groups in the polysiloxane-bound ether–phosphine ligands **1a′(Q■)₂–1c′(Q■)₂** and **1a′(Q■)₁₀** do not meet this condition because cross polarization and proton relaxation in the rotating frame occur at similar rates [e.g., for **1a′(Q■)₂**, T_{SiH} = 2.77 ms and $T_{1\rho H}$ = 2.47 ms, see the Experimental Section and Table 2]. In the case of the polysiloxane-bound complexes ($T_{1\rho H}$ = 5.4–5.5 ms, see Table 2), the determination of I_0 of the silyl species by CP-MAS NMR spectroscopy is exemplarily presented in Table 1 for **3b′(Q■)₆**. The "calculated" real amounts I_0 have been compared to the "absolute" areas of a ^{29}Si MAS NMR spectrum (SPE) in Table 1. Although the accuracy of quantitative ^{29}Si CP-MAS NMR has been generally estimated to be approximately ±10%,[18,26] both methods are in acceptable agreement. Since the expected ratio of T:Q = 1:2 of the polysiloxane matrix has been verified by both methods, domains related to silica gel with "bulk" Q^4 species seem to be absent. Moreover, the discrepancy in the I_0 values of the T and Q type silicon species between the CP and the SPE methods is within this margin of error. Therefore, the T-functionalized (ether–phosphine)ruthenium moieties and the Q species in **3b′(Q■)₆** cannot be phase separated or located in domains of either T or Q groups but have to be totally mixed in the material. Fyfe and co-workers have recently shown by a two-dimensional ^{1}H/^{29}Si correlation experiment, that the Q species in a methyl-substituted, D_2O-treated gel have been directly cross polarized from the methyl group of the T species in a considerable amount.[14] Thus the components are mixed in the gel and this is in excellent agreement with our studies.

In Table 2, various samples prepared by the methods 1, 2a,b, and 3 have been listed with their relative content of silyl moieties I_0. In the ^{29}Si solid-state NMR spectra of the polysiloxane-bound ether–phosphine ligands, no T^1 and only low amounts of T^2 species have been detected. This is reflected in a high degree of condensation[20] for the T groups (91–94%). T moieties of the complexes prepared by methods 1 and 2a also show a high degree of condensation (79–86%), which is one basic requirement for an application in catalysis without leaching of the T species and the ruthenium complexes, respectively. The degree of condensation of the Q silicon species in samples prepared by the methods 1 and 2a (Table 2) shows negligible tolerances (±2%). In each of the polysiloxane-bound complexes prepared by method 1, the anticipated ratio of T:Q has been found by quantification with CP excitation, except for sample **3b′(Q■)₃₀**. In this case, just 67% of the Q^4 silicon species, found by ^{29}Si MAS NMR spectroscopy (SPE), were determined by the cross polarization method. The presence of a considerable amount of "bulk" Q^4 groups in this case indicates the formation of domains *related to silica gel, which are at least 1–2 nm in diameter.*

Ether–phosphine complexes prepared by method 2a show a lower content of Q silicons. 25–45% of the total amount of Q groups were removed as uncondensed silicic acid or oligomers during the precipitation and washing process. The degree of condensation is similar for T and Q species and somewhat lower compared to complexes obtained by method 1. The $T_{1\rho H}$ data of the polysiloxane matrix in the samples prepared by method 2a also show a single exponential behavior and are uniform for the T and Q silicons, too. The values are comparable to those found for the polysiloxane-bound complexes prepared according to method 1 (Table 2). Thus, in principle, the polymer network obtained by both methods should not differ. For the samples

---

(28) Léonardelli, S.; Facchini, L.; Fretigny, C.; Tougne, P.; Legrand, A. P. *J. Am. Chem. Soc.* **1992**, *114*, 6412–6418.

(29) Walther, K. L.; Wokaun, A.; Baiker, A. *Mol. Phys.* **1990**, *71*, 769–780.

Table 2. Quantification of Materials Prepared by Methods 1, 2a,b and 3 by ^{29}Si Solid-State NMR Spectroscopy

		relative I_0 data of T and Q species						found	degree of condensation (%)		degree of hydrolysis (%)	
compound	$T_{1\rho H}$ (ms)^a	T^1	T^2	T^3	Q^2	Q^3	Q^4	T:Q	T	Q	T	Q
						Method 1						
1a′(Q^n)	2.47		1.9	8.1	1.6	8.7	7.9	1:1.82	94	84	100	
1a′(Q^n)$_{10}$^{b}	3.61		2.1	7.9	6.8	46.1	40.7	1:9.36	93	84	98	
1b′(Q^n)$_2$^{b}	3.72		2.8	7.2	2.2	10.8	8.5	1:2.15	91	82	100	98
1c′(Q^n)$_2$^{b}	3.96		2.2	7.8	1.9	8.9	8.6	1:1.94	93	84	100	97
3a′(Q^n)$_6$^{c}	5.5	0.6	3.0	6.4	2.1	9.3	8.3	1:1.97	86	83	96	
3b′(Q^n)$_6$^{c}	5.4	0.5	3.1	6.4	2.0	9.4	8.7	1:2.01	86	83	100	100
3c′(Q^n)$_6$^{c}	5.4	1.0	3.1	5.9	2.7	9.6	7.6	1:1.99	83	81	96	99
3c′(Q^n)$_{10}$^{c}	5.4	1.5	2.5	6.0	4.2	17.8	11.9	1:3.39	82	81	97	98
3c′(Q^n)$_{30}$^{c}	5.4–20^d	0.7	2.8	6.5	15.2	43.5	29.6^{e,f}	1:8.83^{e,f}	86	82	100	99
						Method 2a						
3a′(Q^n)$_{3.4}$^{c}	5.5	1.7	3.0	5.3	1.7	5.2	4.4	1:1.13	79	81	98	
3b′(Q^n)$_{4.4}$^{c}	5.5	1.1	3.4	5.5	1.9	7.2	5.5	1:1.46	81	81	100	100
3c′(Q^n)$_{4.2}$^{c}	5.4	1.2	3.8	5.0	1.9	6.9	4.8	1:1.41	79	80	98	100
						Method 2b						
Mg^{2+}–3a′(Q^n)$_3$^{c}	5.4	1.5	3.8	4.7	1.5^g	4.6	3.1	1:0.99	78	76	89	
Mg^{2+}–3c′(Q^n)$_6$^{c}	5.4	1.4	3.6	5.0	4.3^h	7.6	5.2	1:1.94	79	73	92	100
						Method 3						
silica gel^c	40.5				0.6	4.3	6.3^e			88		100
3c′–silica gel^c	5.5–32^d	2.2^i	5.3	1.0	0.9	4.3	8.0^{e,k}	1:1.32^{e,k}	53	88	89	100

^{a} Determined via ^{29}Si. ^{b} Values from deconvoluted ^{29}Si MAS NMR (SPE) spectra. ^{c} Values determined by the cross polarization method (Experimental Section). ^{d} At least two components of $T_{1\rho H}$. ^{e} Q^4 moieties maximal four bonds from protons. ^{f} Value determined by a ^{29}Si MAS NMR (SPE) spectrum, I_0 = 43.9 (T:Q = 1:10.03). ^{g} Additional signal, Q$^{2'}$ (I_0 = 1.5). ^{h} Additional signals, Q$^{1'}$ (I_0 = 0.3), Q$^{2'}$ (I_0 = 2.0). ^{i} Additional signal, T^0 (I_0 = 1.5). ^{k} Value determined by a ^{29}Si MAS NMR (SPE) spectrum, I_0 = 14.4 (T:Q = 1:1.96).

prepared by the methods 1 and 2a (Table 2) the degrees of hydrolysis[30] as determined by the residual –OCH$_3$ and –OCH$_2$– signals in the ^{13}C CP-MAS NMR spectra (50.3 and 59.8 ppm, respectively) range between 96 and 100%. Hence, in these cases, nearly all the uncondensed Si functions are polar SiOH groups.

In the sample **3c′–silica gel**, which was obtained by "heterogeneous polycondensation" according to method 3 (T:Q ≈ 1:2), the condensation reaction of the T-functionalized ruthenium complexes during the sol–gel process was less efficient. Even uncondensed T^0 species at –43.2 ppm have been observed in the ^{29}Si CP-MAS NMR spectrum (Table 2). The low degree of condensation of 53% can be explained in terms of the lack of suitable Q-copolymerization partners and isolated T^0 functions[1,10] in the expected T–T/Q–Q material. These experiments demonstrate that a *high degree of condensation of the T-functionalities* can solely be obtained by *a simultaneous cocondensation of T with Q moieties starting from the monomers* according to methods 1 and 2. This is necessary for a good fixing of the ruthenium complexes in the gel matrices in view of a successful application as a stable, heterogeneous catalyst.

As a result of the quantification, the averaged structure of the polysiloxane matrix of the ether–phosphines and their ruthenium complexes prepared by the methods 1 and 2a [Table 2, except sample **3c′(Q^n)$_{30}$**] can be visualized. Fifty to sixty percent of the matrix consist of mixed T^3 and Q^3 species, which form a two-dimensional layer structure. Incorporated Q^4 species (25–30%) as elements of the three-dimensional network cross-link these layers. Smaller amounts of T^2 and Q^2 species are random elements of the disordered layers or are included as chain segments. In the case of the complexes, three T-functionalized (ether–phosphine) moieties are additionally linked by a ruthenium atom. Thus, the main parts of the silicon building blocks in the polysiloxane matrices (70–75%) are one- and two-dimensional elements.

^{31}P and ^{13}C CP-MAS NMR Spectroscopy. In the ^{31}P CP-MAS NMR spectra of the polysiloxane-bound ether–phosphines **1a′(Q^n)$_2$–1c′(Q^n)$_2$**, one signal has been observed. The chemical shifts are comparable to those observed by ^{31}P{^{1}H} NMR spectroscopy of the monomers in solution. In Table 3, the ^{31}P signals of the polysiloxane-bound O,P-ligands **1a′(Q^n)$_2$–1c′(Q^n)$_2$** are listed together with their corresponding P-coordinated complexes **3a′(Q^n)$_6$–3c′(Q^n)$_6$**. No free ether–phosphine ligands, but the signals of *trans*-P^2 and *cis*-P^1 (Scheme 1) with the relative intensities of 2:1, are observed in the spectra. Since *all* ether–phosphine ligands are P-coordinated to ruthenium, each T moiety of the ligand contains one-third of the ruthenium complex fragment HRuCl(CO). The ^{31}P and ^{13}C chemical shifts and the C≡O absorption in the IR spectra of the polysiloxane-bound complexes are in agreement with those of their monomeric counterparts (see the Experimental Section). The ^{31}P CP-MAS NMR spectra of the monomeric complex **3c** (Figure 3A) and the polysiloxane-bound complex **3c′(Q^n)$_6$** (Figure 3B) show that sol–gel processing with Si(OEt)$_4$ does not change the complexes, but increases the line widths of the signals of P^2 and P^1 due to an enhanced dispersion of the chemical shifts of the phosphorus nuclei.

Table 3. δ ^{31}P, T_{PH}, $T_{1\rho H}$, and T_{1P} Data for **1a′(Q^n)$_2$–1c′(Q^n)$_2$** and **3a′(Q^n)$_6$–3c′(Q^n)$_6$**

compound	δ ^{31}P (ppm)	T_{PH} (ms)	$T_{1\rho H}$	T_{1P} (s)
1a′(Q^n)$_2$	–32.9	0.58	2.93	5.2
1b′(Q^n)$_2$	–32.5	0.23	4.42	6.9
1c′(Q^n)$_2$	–34.9	0.24	4.90	10.5
3a′(Q^n)$_6$	17.3 (P^2), –0.3 (P^1)	0.21 (P^2), 0.22 (P^1)	5.83	7.0 (P^2), 7.0 (P^1)
3b′(Q^n)$_6$	18.5 (P^2), –1.3 (P^1)	0.16 (P^2), 0.17 (P^1)	6.05	13.9 (P^2), 13.6 (P^1)
3c′(Q^n)$_6$	20.1 (P^2), 1.9 (P^1)	0.17 (P^2), 0.19 (P^1)	6.17	11.6 (P^2), 11.4 (P^1)

The mobilities of the ether–phosphines and their ruthenium complexes in the polysiloxane framework have been studied by ^{31}P CP-MAS NMR spectroscopy. The free ether–phosphine ligands **1b′(Q^n)$_2$** and **1c′(Q^n)$_2$**, containing tetrahydrofuryl and 1,4-dioxanyl groups, magnetize faster (lower T_{PH} constants) than methoxyethyl-substituted **1a′(Q^n)$_2$** (see Table 3). The line widths of the ^{31}P signals of the samples **1a′(Q^n)$_2$**, **1b′(Q^n)$_2$**, and **1c′(Q^n)$_2$** are 640, 870, and 1160 Hz, respectively. Moreover, $T_{1\rho H}$ and T_{1P} relaxation times are featured by an increase in this series. Thus, decreasing mobilities in the free ether–phosphine ligands from **1a′(Q^n)$_2$** to **1b′(Q^n)$_2$** and **1c′(Q^n)$_2$** are evident. When the phosphine ligands are bound to ruthenium, the phosphorus nuclei

---

[30] Degree of hydrolysis of the T species = (1 – n/3)100, degree of hydrolysis of Q species = (1 – n/4)100; n = number of residual OCH$_3$ (T species) or OCH$_2$ groups (Q species) per silicon atom.

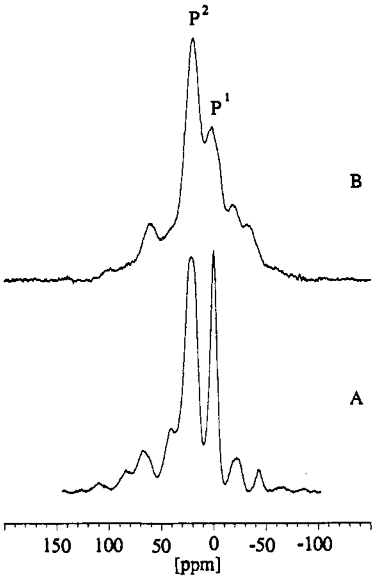

Figure 3. Solid-state ^{31}P CP-MAS NMR spectra of **3c** (A, 3.5 kHz) and after sol–gel processing with $Si(OEt)_4$ [B, **3c′**$(Q^n)_6$, 3.2 kHz]. The broadened signal of P^2 in A is due to diastereomers.

Table 4. $\delta^{13}C$, T_{CH}, $T_{1\rho H}$, and T_{1C} Data for **1a′**$(Q^n)_2$ and **3a′**$(Q^n)_6$

carbon	δ ^{13}C (ppm)	T_{CH} (ms)	$T_{1\rho H}$ (ms)	T_{1C} (s)
		a. **1a′**$(Q^n)_2$		
C-1	13.9	0.189	2.46	1.25
C-2	18.3	0.114	2.55	1.14
C-3,5	27.2	0.165	2.68	0.54
C-6	70.0	0.251	2.51	0.86
C-8	58.2	0.350	2.38	1.76
C-*i*	139.5	0.140	2.44	2.64
C-*o*	132.1	0.203	2.43	1.09
C-*m,p*	128.7	0.179	2.42	0.84
		b. **3a′**$(Q^n)_6$		
C-1	14.1	0.182	5.35	3.80
C-2	17.9	0.182	5.97	4.70
C-3,5	27.3	0.158	5.85	4.81
C-6	68.5	0.165		3.61
C-8	57.9	0.725	5.48	3.75
C-*o,m,p*	129.4	0.289	5.63	6.36

are cross polarized faster (T_{PH} constants decrease), while the relaxation times $T_{1\rho H}$ and T_{1P} (Table 3) and the chemical shift anisotropy increase. This is due to the expected reduced mobilities of the polysiloxane-bound ligands upon coordination to the ruthenium atom. The magnetization in the T_{1P} experiment of the (ether-phosphine)ruthenium complexes **3a′**$(Q^n)_6$–**3c′**$(Q^n)_6$ showed a multiexponential decrease of the signal intensities, which was approximated by a biexponential function. The amount of the "two" components has been taken into account with their T_{1P} times to give one averaged T_{1P} value (Table 3). In contrast, the magnetization in the T_{1P} experiments of each of the free ether-phosphines **1a′**$(Q^n)_2$–**1c′**$(Q^n)_2$ showed a single-exponential behavior. This is due to the mobilities of the free ether–phosphine ligands, which average different local environments of the polysiloxane materials.

In Figure 4, $T_{1\rho H}$ and T_{1P} of the ether–phosphine ligands **1a′**$(Q^n)_2$–**1c′**$(Q^n)_2$ (Figure 4A–C) and the complex **3a′**$(Q^n)_6$ (Figure 4D,E) are shown as a function of the temperature. In the very mobile free ligand **1a′**$(Q^n)_2$, the increase in temperature is correlated with increasing $T_{1\rho H}$ values (Figure 4A). However, in the case of the bulky, free ether–phosphines **1b′**$(Q^n)_2$ and **1c′**$(Q^n)_2$, decreasing $T_{1\rho H}$ values were determined by increasing the temperature, until minima at 337 K (1.83 ms) and 357 K (2.19 ms), respectively, were reached (Figure 4A). In all samples of **1a′**$(Q^n)_2$–**1c′**$(Q^n)_2$, the T_{1P} times (Figure 4B) and the line widths of the peaks in the ^{31}P CP-MAS NMR spectra (Figure 4C) decreased to a range of similar values (2.5–3.1 s and 234–374 Hz, respectively). The low T_{1P} data of the free ether–phosphines above 357 K are close to those of phosphines in liquids at ambient temperature. These studies clearly demonstrate the temperature-dependent transition of the ether–phosphines *in the gel* to very mobile ligands. The high mobility behavior enables the reversible exchange of P^1 in the polysiloxane-bound ruthenium complexes $HRuCl(CO)(P{\sim}O)_3$ with a CO ligand above 60–70 °C.[10] In the complex **3a′**$(Q^n)_6$, the temperature dependence of $T_{1\rho H}$ and T_{1P} is completely different, the effects being much smaller (Figure 4, parts D and E, respectively). First of all, $T_{1\rho H}$ and T_{1P} decreased slightly. Above 320 K, increasing $T_{1\rho H}$ values of P^1 and P^2 in the complex have been observed (Figure 4D). The T_{1P} curve showed a sudden drop to lower values between 320 and 340 K (Figure 4E), and the line width of P^2 in the ^{31}P CP-MAS NMR spectra of the complex decreased reversibly from 1400 to 1200 Hz. The ^{31}P CP-MAS NMR spectra of **3a′**$(Q^n)_6$ at 367 and 297 K are shown in Figure 5.

Above 347 K, the magnetization decay in the T_{1P} experiment of the P nuclei in the ruthenium complex showed a single-exponential behavior. This indicates, that the ruthenium complex is fixed nonrigidly by its three carbon spacers to the matrices within the gel. At room temperature, the complex has given rise to a ^{31}P CP-MAS NMR spectrum similar to that recorded at 367 K (Figure 5A) after it was treated with a small amount of methanol to induce swelling. Both the change of temperature and the adsorption of methanol lead to a smaller dispersion of the chemical shifts of the phosphorus nuclei due to the *nonrigid behavior* of the polysiloxane systems. The chemical shift anisotropy in the complex remained unchanged, which is consistent with a limited effect of temperature on the relaxation time T_{1P} (Figure 4E) and strong, rigid Ru–P bonds. Thus, the transition in the T_{1P} curves of the dry sample is caused by a thermal change in the material which might be related to the glass transition of organic polymers.[23]

The corresponding dynamic parameters obtained from ^{13}C CP-MAS NMR spectra of the same system at 297 K are listed in the Table 4a,b. In agreement with the results obtained by ^{31}P solid-state NMR spectroscopy, $T_{1\rho H}$ and T_{1C}, evaluated from ^{13}C CP-MAS NMR spectra, show higher values in the complex **3a′**$(Q^n)_6$ than in the free ligand **1a′**$(Q^n)_2$. The $T_{1\rho H}$ data in both samples are in the range of those determined via the ^{29}Si (see Table 2) and ^{31}P nuclei (see Table 3). Due to the low natural abundance of ^{13}C nuclei, the spin diffusion process between them is minimal and different carbons exhibit different T_{1C} relaxation times (Table 4a,b).[22] Thus decreasing T_{1C} data in **1a′**$(Q^n)_2$ were obtained from C-1 to C-2 and C-3,5, showing the increasing mobilities of the carbons along the spacer. The higher values for the T_{1C} relaxation time (1.76 s) and the T_{CH} constant (350 μs) of the terminal methoxy group in **1a′**$(Q^n)_2$ indicate a methyl group rotation in the free ligand.[31]

The solid-state NMR investigations elucidate the thermal properties and the behavior of mobility of the functional centers in the polysiloxane material with a T:Q ratio of 1:2. All polysiloxane-bound ether–phosphines drastically increase their mobility in the gel when the temperature is raised. In contrast, coordinated ether–phosphines are strongly bound to ruthenium although the materials show a nonrigid character when the temperature has been increased. Therefore this tailoring of a functionalized material can be considered as an intermediate system between a solution and a solid and should combine the advantages of homogeneous and heterogeneous catalyses.

Relationship to Silica Gel Attached Systems. Silica gels normally show much higher $T_{1\rho H}$ values (typically 20–50 ms[24,32]) than those reported in this work for functionalized polysiloxanes (Tables 1 and 2). Thus, if more $Si(OEt)_4$ is used for the

---

(31) Sindorf, D. W.; Maciel, G. E. *J. Am. Chem. Soc.* **1983**, *105*, 1848–1851.

(32) Maciel, G. E.; Sindorf, D. W. *J. Am. Chem. Soc.* **1980**, *102*, 7607–7608.

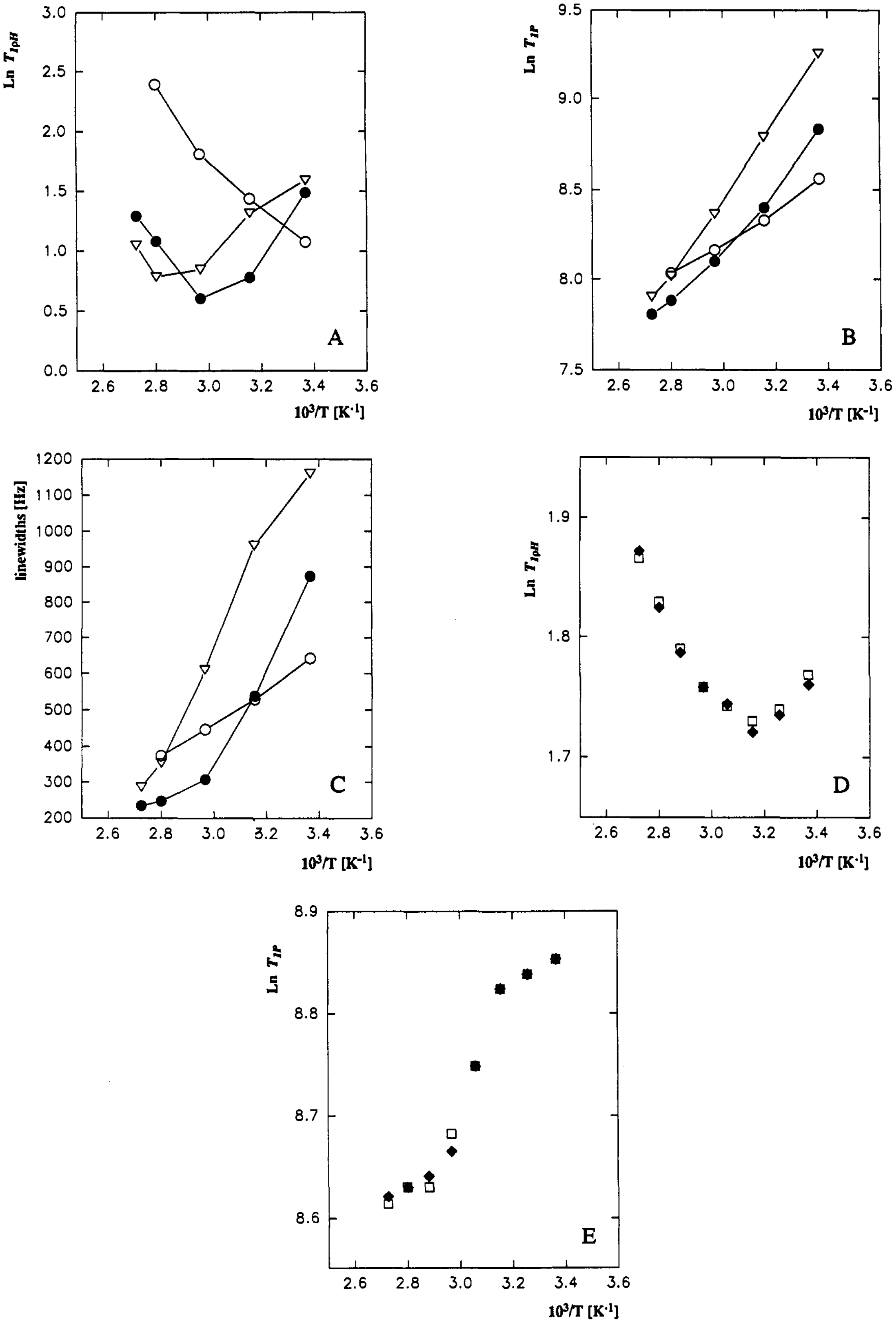

Figure 4. $T_{1\rho H}$ (A), T_{1P} (B), and line widths (C) of the polysiloxane-bound ether–phosphine ligands **1a'**$(Q^n)_2$ (○), **1b'**$(Q^n)_2$ (●), and **1c'**$(Q^n)_2$ (▽) as functions of the temperature. $T_{1\rho H}$ (D) and T_{1P} (E) of the P-coordinated ether–phosphine ligand in **3a'**$(Q^n)_6$ as functions of the temperature (□, P^2; ◆, P^1).

cocondensation, it should be possible to find out the transition when silica gel domains are formed due to an inhomogeneous molecular mixing between the T and Q functionalities.

For the silica gel sample (Figure 6A, method 3), the Q species show a $T_{1\rho H}$ value of 40.5 ms. After the cocondensation with **3c** to form **3c'–silica gel** (T:Q ≈ 1:2, method 3), the Q species show the expected two components of $T_{1\rho H}$ (Figure 6B). The lower value is comparable with that calculated from the single-exponential magnetization decay of the signals of the T groups (T^1 and T^2) in this sample (5.5 ms); the larger one is in the range

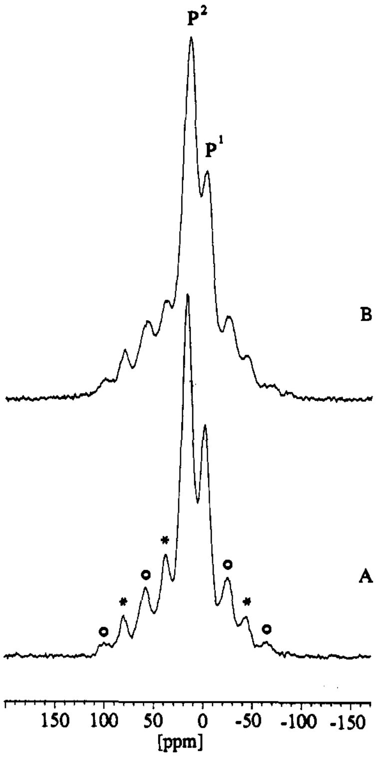

Figure 5. Solid-state ^{31}P CP-MAS NMR spectra (3.4 kHz) of **3a′**$(\mathrm{Q}^{\bullet})_6$ at 367 (A) and 297 K (B).

19–33 ms. The majority of the protons (≈70%) of the Q^3 species in **3c′–silica gel** show the low $T_{1\rho H}$ value; hence they are dipolar-coupled with the protons of the T domains. Q^3 protons with longer $T_{1\rho H}$ values are located in the bulk of the silica gel domains, separated and less influenced by "surface" T and Q protons (see Table 2). Therefore, this sample consists of domains formed by the T groups of the ruthenium complexes **3c′** and a core of rigid silica gel, as it is expected from the preparation according to method 3.

In contrast to **3c′–silica gel**, the samples **3c′**$(\mathrm{Q}^{\bullet})_{30}$ and **1a′**$(\mathrm{Q}^{\bullet})_{10}$ were prepared by homogeneous copolymerization (T:Q = 1:10, method 1). Figure 6C shows the $T_{1\rho H}$ behavior of **3c′**$(\mathrm{Q}^{\bullet})_{30}$, which is comparable to that described in the previous sample. Those protons which are located in close proximity to the complexes show one low $T_{1\rho H}$ component of 5.4 ms. This is demonstrated by a measure of $T_{1\rho H}$ via the sensitive ^{31}P probe and the ^{29}Si nuclei of the T^3 species in **3c′**$(\mathrm{Q}^{\bullet})_{30}$. Hence, 70–80% of the protons bound to Q species are dipolar-coupled with these fast relaxing protons, but 20–30% show components between 18 and 20 ms. However, the $T_{1\rho H}$ behavior of the protons in the polysiloxane matrix of the ether–phosphine ligand **1a′**$(\mathrm{Q}^{\bullet})_{10}$ (T:Q = 1:10 as above) is single exponential and similar for both T and Q species (3.61 ms, Figure 6D).

We conclude that the sample **3c′**$(\mathrm{Q}^{\bullet})_{30}$ (Figure 6C) consists of domains, with high and low densities of the T-functionalized ruthenium complexes, whereas the distribution of the T functionalities in **1a′**$(\mathrm{Q}^{\bullet})_{10}$ is homogeneous, making the dipolar coupling of the protons efficient across the whole sample. This indicates that hydrolysis and condensation steps in the complex **3c**, which has been equipped with three T functions in one unit, is preferred compared to Si(OEt)$_4$ or **1a–c** containing one Q and one T unit, respectively. This can be explained by the formation of gels of **3a–c** in alcohols at much lower concentrations than observed with Si(OEt)$_4$ and **1a–c**. Hence, the concentration of Si(OEt)$_4$ or hydrolysis products increases, leading to the formation of Q-domains related to silica gel during the proceeding sol–gel reaction. This is in agreement with experimental observations: when the gel process is stopped after 2 h, the T-functionalized ruthenium complex is immobilized quantitatively, but a considerable amount of Si(OEt)$_4$ is washed out.

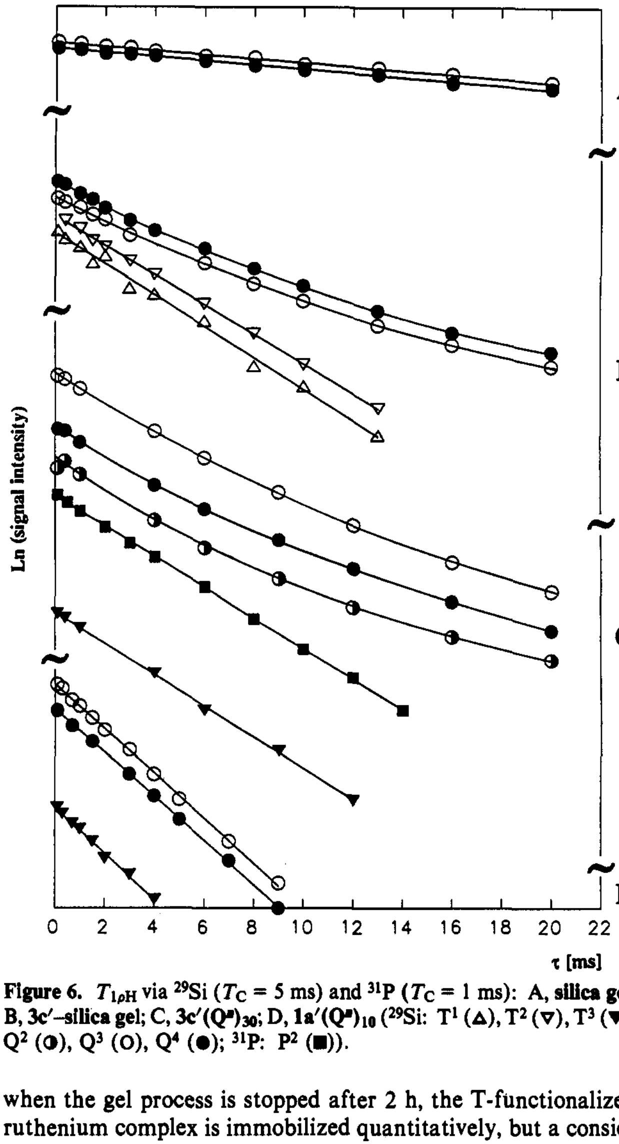

Figure 6. $T_{1\rho H}$ via ^{29}Si (T_C = 5 ms) and ^{31}P (T_C = 1 ms): A, **silica gel**; B, **3c′–silica gel**; C, **3c′**$(\mathrm{Q}^{\bullet})_{30}$; D, **1a′**$(\mathrm{Q}^{\bullet})_{10}$ (^{29}Si: T^1 (△), T^2 (▽), T^3 (▼), Q^2 (◑), Q^3 (○), Q^4 (●); ^{31}P: P^2 (■)).

Summing up, these investigations show the transition of the matrix to *silica gel related domains* when more than 10–30 equiv of Si(OEt)$_4$ are involved in the sol–gel process with **3a–c** according to method 1 or if the two-step process (method 3) is applied. Therefore, those matrices of the ruthenium complexes listed in Table 2 with T:Q ratios up to 1:3.3, prepared by the methods 1 and 2a,b, can generally be defined as uniform systems, whereas the samples **3c′**$(\mathrm{Q}^{\bullet})_{30}$ (T:Q = 1:10, method 1) and **3c′–silica gel** (T:Q ≈ 1:2, method 3) cannot.

Polysiloxane Matrices Doped with Mg^{2+} Cations. The ^{29}Si CP-MAS NMR spectrum of **3c′**$(\mathrm{Q}^{\bullet})_6$, polycondensated by the addition of MgSO$_4$ according to method 2b, is shown in Figure 7. The material contained 1.04 wt % Mg^{2+} cations. While the chemical shifts of the T, Q^2, Q^3, and Q^4 species and the $T_{1\rho H}$ behavior in the sample remained similar to those of the Mg^{2+}-free counterparts, additional signals at −81.0 and −86.5 ppm have been found in the spectrum. They can be interpreted as Q$^{1'}$ and Q$^{2'}$ species, in which one SiOH proton has been exchanged with a Mg^{2+} cation.[33,34] This is in agreement with the correspondence of the sum of the Q$^{1'}$ and Q$^{2'}$ species with the amount of Mg^{2+} cations per unit. The Mg^{2+} ions, which are bound exclusively to Q species, somewhat lower the degree of condensation of the Q type silicon species (see Table 2). Thus, the polysiloxane matrix

---

(33) Lippmaa, M.; Mägi, M.; Samoson, A.; Engelhardt, G.; Grimmer, A.-R. *J. Am. Chem. Soc.* **1980**, *102*, 4889–4893.

(34) Rocha, J.; Welch, M. D.; Klinowski, J. *J. Am. Chem. Soc.* **1991**, *113*, 7100–7103.

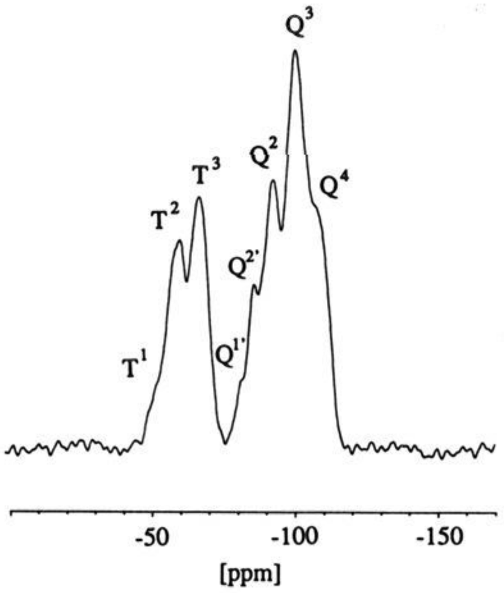

Figure 7. Solid-state ^{29}Si CP-MAS NMR spectrum of Mg^{2+}-doped **3c′(Q^n)$_6$** prepared by method 2b.

and the distribution of the ruthenium complexes therein can be compared to the respective Mg^{2+}-free samples.

Summarizing the solid-state NMR investigations, novel, uniform, and homogeneous materials have been classified, which unify both "inorganic" and "organic" properties, if the copolymerization of the T and Q species has been carried out simultaneously starting from monomers with low amounts of $Si(OEt)_4$: the T_{SiH} constants of the Q groups can be well compared to those of native silica gels, whereas their extremely low, uniform $T_{1\rho H}$ values and the temperature behavior, the quantities of $T_{1\rho H}$ via ^{13}C and ^{31}P, T_{1C}, T_{CH}, and T_{1P}, are typical of organic polymers or related systems. These properties can be explained by the fact that the T moieties of the ruthenium complexes and the ether–phosphine ligands are substantial building blocks of the support being interpenetrated with Q species to form a suitable, flexible organic–inorganic hybride catalyst system. If more equivalents of $Si(OEt)_4$ or native silica gel are involved in the sol–gel process with the ruthenium complexes **3a–c**, the resulting materials are not uniform and should therefore differ in their catalytic properties.

Surface Structures of the Materials. The surface areas (BET) of the samples prepared according to methods 1, and 2a,b lie between 1 and 18.5 m^2/g. These low values are in the range of the external surface of the gel particles. This agrees with SEM micrographs, which show nonporous surfaces of the gels. The materials prepared by method 1 [e.g. **3c′(Q^n)$_6$** in Figure 8 (top)] are aggregates of irregular shapes (lumps) and show crushed gel particles with size distributions in the range 5–30 μm. However, precipitation according to method 2a resulted in more uniform, tiny, and rounded particles [e.g. **3c′(Q^n)$_{4.2}$** in Figure 8 (bottom)]. Samples prepared by method 2b, which contained low amounts of Mg^{2+}, showed a more structured, but nonporous, surface with small particle sizes of 0.5–5 μm.

The surface area of silica gel (method 3) was determined to 180 m^2/g, and the SEM micrographs showed a porous surface as expected (particle size distribution of 10–30 μm). After the sol–gel process of silica gel with **3c** to form **3c′–silica gel** (T:Q ≈ 1:2), the surface area decreased and huge, nonporous particles (SEM = 30–50 μm) formed. This coating of silica gel by a shell of **3c′** without Q species is in agreement with the low degree of condensation of the T-functionalized ruthenium complex moieties, the amount of "bulk" Q^4 species (see Table 2), and the $T_{1\rho H}$ behavior (Figure 6).

From the sample **3b′(Q^n)$_6$** with a total degree of hydrolysis of 100%, the molecular water, being adsorbed at "surface" silanol groups, has been determined to 3.11% by the Karl Fischer method.[35] This corresponds to 0.278 water molecules per silicon atom—approximately half the amount of the concentration of silanol groups in the matrix (an average of 0.58 OH/Si)—and indicates that *two* of the silanol groups are associated to *one* water molecule. Thermal gravimetric and Karl Fischer analysis showed that the adsorbed water has been lost after treatment at 100 °C, while no further condensation of the matrix was detectable by ^{29}Si CP-MAS NMR spectroscopy. Although molecular water had been removed, the IR spectra of **3b′(Q^n)$_6$** showed no free SiOH vibrations at 3700–3750 cm^{-1},[36] but the broad absorption band of associated SiOH···(H)OSi hydroxyl groups[36] at 3200–3600 cm^{-1}. Subsequently the sample was exposed to methanol vapor. Considerable swelling was induced, and a sharp signal at 49.5 ppm (line width of 28 Hz) appeared in the ^{13}C CP-MAS NMR spectrum (TOSS) due to methanol molecules being adsorbed at "surface" SiOH groups. The amount of adsorbed methanol in **3b′(Q^n)$_6$** was determined to be 0.54 molecules per silicon atom, which is in the range of the concentration of silanol groups (0.58 OH/Si). This indicates that each of the silanol functions are associated to one methanol molecule. The amount of adsorbed organic molecules decreased with their polarity (MeOH, 0.54/Si; EtOH, 0.39/Si; acetone, 0.28/Si; THF, 0.26/Si; Et_2O, 0.08/Si; alkanes, 0.03/Si). These studies indicate that the silanol groups, even in the "bulk" of the polymer network, are accessible to polar organic molecules like methanol. However, swelling has been hardly induced by exposure of the materials to nonpolar molecules because of the strongly bridging hydrogen bonds between the polar silanol groups. This is in agreement with a *convertible "surface"* of the materials. This point of view

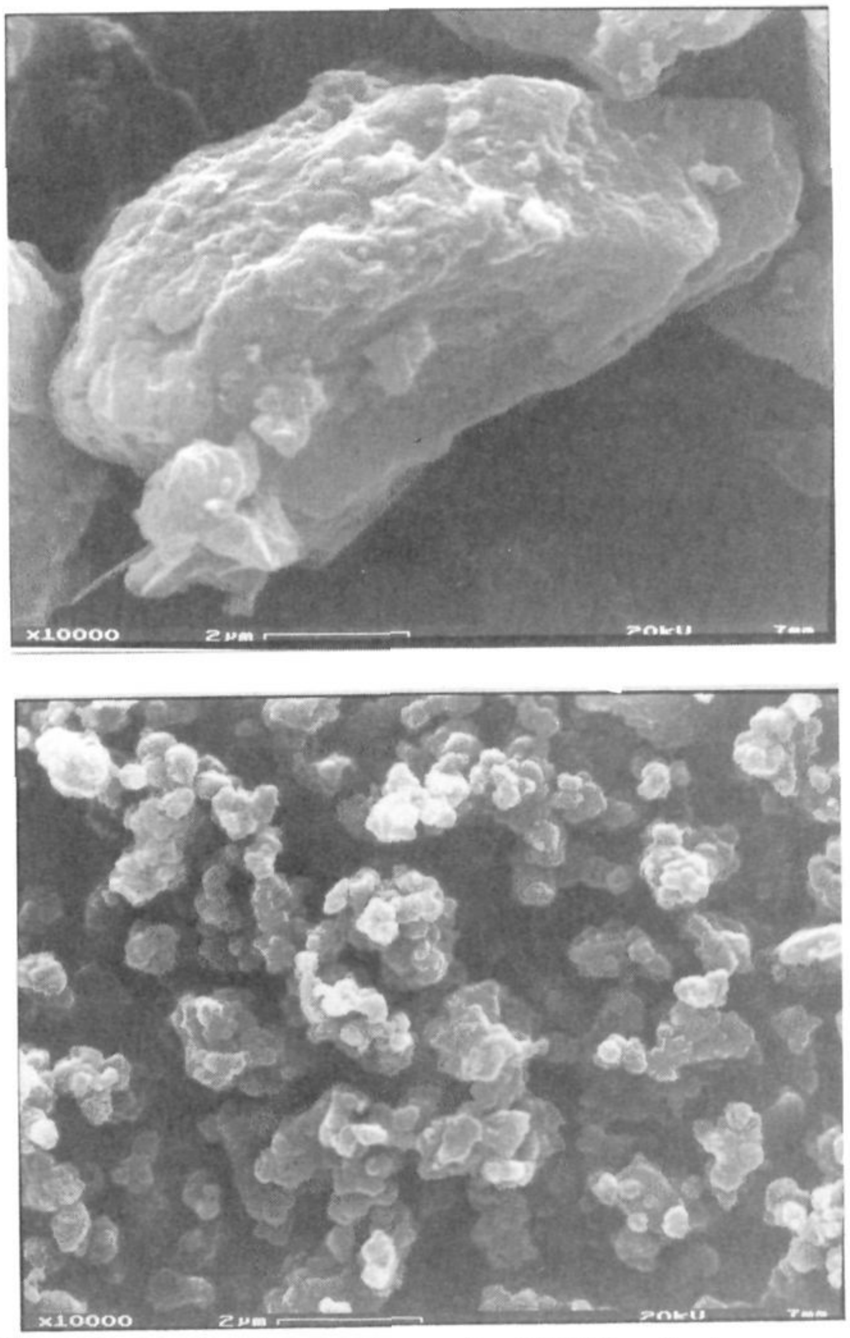

Figure 8. Scanning electron micrographs of **3c′(Q^n)$_6$** sol–gel processed by method 1 (top) and **3c′(Q^n)$_{4.2}$** precipitated according to method 2a (bottom).

---

[35] Scott, R. P. W.; Traiman, S. *J. Chromatogr.* **1980**, *196*, 193–205.

[36] Fischer, H. E.; King, S. A.; Miller, J. B.; Ying, J. Y.; Benziger, J. B.; Schwartz, J. *Inorg. Chem.* **1991**, *30*, 4403–4408.

Table 5. Hydrogenation of *n*-Butyraldehyde

a. Isothermal Hydrogenation[a]

catalyst	surface area (m^2/g)	particle size (μm)	temp (°C)	reaction time[b] (min)	conversion (%)	turnover freq (min^{-1})
			Method 1			
$\mathbf{3a'}(Q^n)_6$[c]	5–9	5–15	50	60	16.5	2.8
			80	60	62.2	10.4[d]
			100	60	81.1	13.5
			150	45	99.5	22.1
$\mathbf{3b'}(Q^n)_6$[e]	1–10	10–20	50	60	2.4	0.04
			100	60	16.5	2.8
			150	55	98.5	18.0[f]
$\mathbf{3c'}(Q^n)_6$	1–12	5–12	100	60	32.5	3.9
			150	45	100	22.2[g]
$\mathbf{3c'}(Q^n)_{10}$	7–11	10–30	150	60	91.8	15.3
$\mathbf{3c'}(Q^n)_{30}$	14	20–30	150	60	74.9	12.5
			Method 2b			
Mg^{2+}–$\mathbf{3c'}(Q^n)_6$[h]	3–8	0.5–5	150	15	100	66.6[i]

b. Nonisothermal Hydrogenation[j]

catalyst	surface area (m^2/g)	particle size (μm)	reaction time[k] (min)
	Method 2a		
$\mathbf{3a'}(Q^n)_{3.4}$	13.5	1–2	4–5
$\mathbf{3b'}(Q^n)_{4.4}$	18.5	1–1.5	4–5
$\mathbf{3c'}(Q^n)_{4.2}$	10.0	0.5–2	4–5[l]
	Method 2b		
Mg^{2+}–$\mathbf{3a'}(Q^n)_3$	11.0	1–4	6–7[m]
	Method 3		
3c'-silica gel	9–15	30–50	2–2.5[n]

[a] Starting H_2 pressure = 50 bar (296 K), Ru:*n*-butyraldehyde = 1:1000, selectivity = 100%. [b] Counted from the point when the reaction mixture in the autoclave has reached the stated temperatures. [c] 7.55% Ru. [d] Second run of 10.0 min^{-1}, 7.76% Ru. [e] 6.83% Ru. [f] Second run of 16.9 min^{-1}, 7.18% Ru; third run of 17.0 min^{-1}, 6.74% Ru. [g] See Figure 9A. [h] 5.95% Ru. [i] Second run of 65.9 min^{-1}, 6.4% Ru. [j] Starting H_2 pressure = 50 bar (296 K), Ru:*n*-butyraldehyde = 1:1000, aldehyde conversion and selectivity = 100%. [k] Estimated from the beginning of the exothermic reaction. [l] See Figure 9B. [m] Reproducible data and constant C, H, Cl, and Ru values during the catalytic runs 1–3 (Experimental Section). [n] Decomposing to a sol of oligomeric ruthenium complexes **3c'** and pure silica gel.

can be explained in terms of the quantitative description of the materials with a T:Q ratio in the range 1:1–1:2 by ^{29}Si solid-state NMR spectroscopy: 70–75% of these matrices consist of flexible chain or folded two-dimensional layer elements, which are anchored by the Q^4 species or the homogeneously divided ruthenium centers in the gel.

The sample $\mathbf{3c'}(Q^n)_{30}$ was hardly swelling in methanol or other solvent vapors (0.31 MeOH/Si compared to the total concentration of silanol groups per silicon of 0.69 OH/Si). This case can be interpreted in terms of a lack in flexibility of the silica gel domains, which partially occlude the silanol groups. The increasing rigidity of the matrices is also evident from decreasing T_{SiH} values of the Q^3 species in the system $\mathbf{3c'}(Q^n)_x$ (amounts of Q species $x = 6$, 10, and 30; $T_{SiH} = 2.01$, 1.66, and 1.42 ms, respectively).

Catalytic Activity of the Materials. The different polysiloxane-bound ruthenium complexes described in this study displayed various interesting properties in hydrogenation of *n*-butyraldehyde to *n*-butanol. In accordance with the literature,[37] the catalytic activity of complexes of the type $HRuCl(CO)(P{\sim}O)_3$ is initiated by cleavage of the ligand P^1 *trans* to H and the coordination of the aldehyde to ruthenium. After treatment with *n*-butyraldehyde, the ether–phosphine ligand $\mathbf{1a'}(Q^n)_2$, which is dissociated from $\mathbf{3a'}(Q^n)_6$ has been observed in the ^{31}P CP-MAS NMR spectrum.

The ether functions in ether–phosphine transition metal complexes can be considered as an intramolecular solvent.[12] They stabilize low coordinated species due to the chelate effect and control a catalytic cycle. This concept was successfully applied in homogeneous catalysis,[12] and the idea is now being extended to polysiloxane materials. Indeed, we have proved that the polysiloxane-bound ether–phosphines show a behavior similar to liquids at higher temperatures: the system should therefore be able to imitate a homogeneous chemical reaction at higher temperatures.

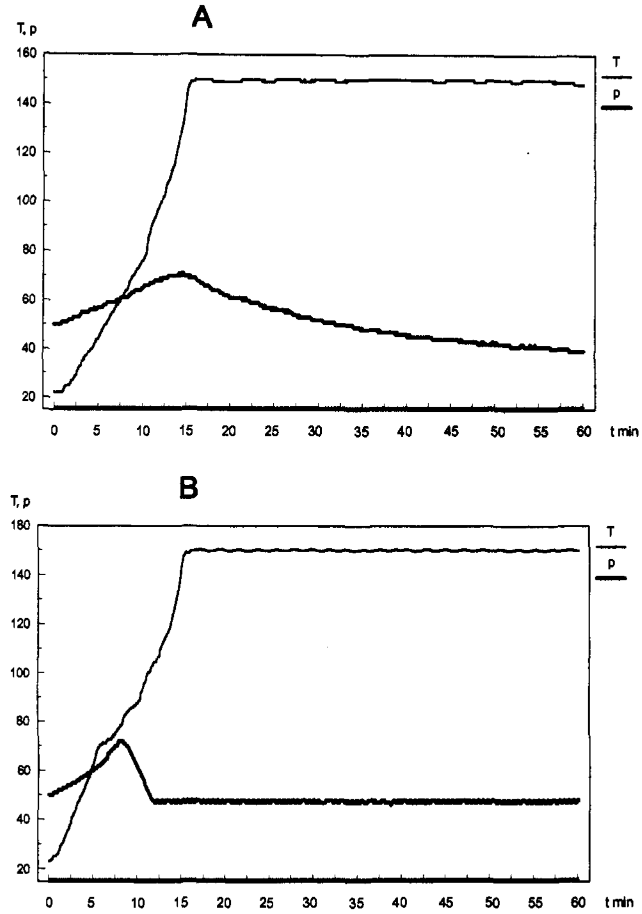

Figure 9. Plot of hydrogenation of *n*-butyraldehyde with polysiloxane-bound $\mathbf{3c'}(Q^n)_6$ prepared by method 1 (A). Plot of hydrogenation of *n*-butyraldehyde with polysiloxane-bound $\mathbf{3c'}(Q^n)_{4.2}$ prepared by method 2a (B).

Catalytic experiments of complexes prepared according to method 1 and the Mg^{2+}-doped sample $\mathbf{3c'}(Q^n)_6$ (method 2b) were carried out isothermally (H_2 pressure at the beginning of the reaction, 50 bar; ruthenium:butyraldehyde = 1:1000, see Table 5a and Figure 9A). In contrast to $\mathbf{3a'}(Q^n)_6$, the samples $\mathbf{3b'}(Q^n)_6$ and $\mathbf{3c'}(Q^n)_6$ proved no significant catalytic activity at 100 °C or below. This might be due to the higher mobility of the anchored ether–phosphine $\mathbf{1a'}(Q^n)_2$ in contrast to $\mathbf{1b'}(Q^n)_2$ or $\mathbf{1c'}(Q^n)_2$ which was established by ^{31}P CP-MAS NMR relaxometry. At 150 °C, the turnover frequency[38] of the system $\mathbf{3c'}(Q^n)_x$ (method 1) decreased with an increasing particle size and a higher content of cocondensated Q silicon moieties x, although the BET values (external surfaces) do not vary significantly. This can be explained by the occlusion of the ruthenium complexes into rigid, nonswelling silica gel related domains, which make them unavailable for catalysis. However, the catalysts $\mathbf{3c'}(Q^n)_x$ ($x = 10$ or 30) could be recovered quantitatively by centrifugation from the reaction medium. In the Mg^{2+}-doped sample the significant higher turnover frequency can be traced back to a smaller particle size and a lower degree of condensation (see Tables 2 and 5a).

Due to their immense catalytic activity, hydrogenation experiments with some samples prepared according to the method

---

(37) Sánchez-Delgado, R. A.; Valencia, N.; Márquez-Silva, R.-L.; Andriollo, A.; Medina, M. *Inorg. Chem.* **1986**, *25*, 1106–1111.

(38) Turnover frequency = mol of product/(mol of catalyst × 60 min).

2a,b could not be performed isothermally under the same conditions (Table 5b). This is explained in terms of tiny particles (0.5–2 μm), a low content of Q silicon groups (T:Q = 1:1–1:1.5), and a somewhat lower degree of condensation compared to materials prepared by method 1. The aldehyde was quantitatively converted into *n*-butanol within several minutes (range of temperature of 80–140 °C). Between 70 and 80 °C the decrease of the H_2 pressure correlated with an exothermic reaction, which was detected by the thermocouple introduced into the reaction medium [*p*/*T*-curve from **3c′(Q$^{\blacksquare}$)$_{4.2}$**, Figure 9B].

After opening the autoclave, the samples prepared by methods 1 and 2a with a T:Q ratio up to 1:2 were present in the form of a highly dispersed, swollen gel, *in cases where the aldehyde was converted in a considerable amount*. The gels were precipitated from *n*-butanol by the addition of alkanes (yields 70–80%).

This reaction behavior can be explained by the formation of polar *n*-butanol within the gel, followed by swelling and a substantial increase of the gels "surface" during the course of the reaction. The resulting concentration gradient between the aldehyde at the outside and *n*-butanol at the inside of the gels exhibits a rapid diffusion of the reactants to and from the catalytic sites. Therefore the differences in catalytic activities depicted in Figure 9A,B can be interpreted qualitatively by a diffusion controlled reaction.

The hydrogenation behavior (*p*/*T* curve) of the sample **3c′–silica gel** (method 3, Table 5b) is identical with that of the monomeric ruthenium complex **3c**: the material was decomposed into pure silica gel and nonseparable, polymeric ruthenium complexes **3c′**, which carried out a homogeneous hydrogenation. This leaching is the result of the low degree of condensation of the domains formed by the T-functionalized ruthenium complexes (53%).

We have shown, that samples with a high amount of Q species can be well separated from the reaction medium, but suffer from a lower catalytic activity due to the nonflexibility of the matrices and occlusion of the complexes. However, samples with a low content of Q silicons and small particle sizes are highly active, but separation is only possible by the addition of nonpolar solvents. The Mg^{2+}-doped catalysts **3c′(Q$^{\blacksquare}$)$_6$** and especially **3a′(Q$^{\blacksquare}$)$_3$** are featured by a *high catalytic activity and were completely recovered by centrifugation after the hydrogenation experiment* due to the small content of ionic, insoluble magnesium silicates. This design of the polysiloxane matrix therefore unifies the properties of a heterogeneous catalyst with a catalytic activity which is not far from those of their monomeric counterparts.

The polysiloxane-bound catalysts described in this study showed no measurable leaching of ruthenium during the hydrogenation of *n*-butyraldehyde (except **3c′–silica gel**, as described above). Constant analytical values of the materials after several catalytic runs have been found (see Table 5a,b and the Experimental Section), and no loss of chemical activity has been observed with Mg^{2+}-doped **3a′(Q$^{\blacksquare}$)$_3$** or **3c′(Q$^{\blacksquare}$)$_6$**. It is most surprising that the degree of condensation in the polysiloxane matrices has even been increased during the hydrogenation reaction: as an example, the degree of condensation of the T species in catalyst **3c′(Q$^{\blacksquare}$)$_6$** increased from 83 to 92% and in the Mg^{2+} derivative from 79 to 86% during one catalytic run. The T:Q ratios remained constant as well as the elemental analyses.

Conclusion. In this study, we have demonstrated that sol–gel processing opens up the tantalizing prospect of designing new suitable catalyst systems with tailored properties which can be investigated unequivocally by the combination of heteronuclear solid-state NMR spectroscopy, surface characterization, and catalysis. The convenient and mild conditions offered by the sol–gel process for the preparation of modified inorganic networks, have paved the way for the synthesis of a new catalyst system. On the nanometer scale, the degree of interpenetration of the organometallic T moieties with the "inorganic" Q species in the sol–gel routes 1 and 2a,b depends on the ratio of these components. At a low content of "inorganic" Q building blocks, the domain sizes are reduced to a level such that uniform molecular T/Q composites have been formed. As a result of this intimate mixing, these hybride catalysts show unique properties: the flexibility of the carbon spacers and the tailored polysiloxane matrices of the gels allows imitation of the chemical reaction of a homogeneous catalyst.

Experimental Section

Instrumentation. The elemental analyses were carried out on a Carlo Erba analyzer, Model 1106. IR data were obtained on a Bruker IFS 48 FT-IR spectrometer. The solution $^{31}P\{^1H\}$, $^{13}C\{^1H\}$, and ^1H nuclear magnetic resonance (NMR) spectra were recorded on a Bruker AC 80 spectrometer; the frequencies, standards, and temperatures are as follows. $^{31}P\{^1H\}$ NMR: 32.438 MHz, external 85% H_3PO_4 in acetone-d_6, 243 K. $^{13}C\{^1H\}$ NMR: 20.15 MHz, internal standard TMS, 300 K. ^1H NMR: 80.13 MHz, internal standard, TMS, 300 K. The high-frequency-positive convention has been used in reporting all chemical shifts δ (ppm). Mass spectra (field desorption) were acquired on a Finnigan MAT 711A modified by malypen-, Meβ- and Datensysteme (8 kV, 60 °C) and are reported as mass/charge (*m*/*z*).

Monomers. General Procedures. All manipulations were performed under argon by employing the usual Schlenk techniques. Methanol was dried with magnesium and distilled from $Mg(OMe)_2$. Acetone was distilled from $MgSO_4$. *n*-Hexane and toluene were distilled from sodium-benzophenone ketyl. H_2O and $Si(OEt)_4$ (Aldrich) were distilled under argon before use. All solvents were stored under argon. The starting complex $HRuClCO(PPh_3)_3$[19] and the ether-phosphines **1a–c**[39] were synthesized as previously described. $^{13}C\{^1H\}$ NMR data of **1b,c** will be given in detail; those of **1a** have been published elsewhere.[10]

Phenyl(tetrahydrofuranyl-2-methyl)(3-(trimethoxysilyl)propyl)phosphine (1b): $^{31}P\{^1H\}$ NMR (toluene) δ −32.3, −34.8 (2s, diastereomers); $^{13}C\{^1H\}$ NMR ($CDCl_3$) δ 138.9, 138.2 [2 d, ^1J(PC) = 14.6, 14.6 Hz, C-*i*], 132.5, 132.4 [2 d, ^2J(PC) = 19.5, 19.5 Hz, C-*o*], 128.6 (C-*p*), 128.2 [d, ^3J(PC) = 7.1 Hz, C-*m*], 77.1, 76.9 [2 d, ^2J(PC) = 18.3, 18.3 Hz, C-6], 67.4 (C-8), 50.2 ($SiOCH_3$), 35.6, 35.0 [2 d, ^1J(PC) = 10.9, 10.9 Hz, C-5], 32.7 (C-10), 32.3 [d, ^1J(PC) = 9.7 Hz, C-3], 25.7 (C-9), 19.2 [d, ^2J(PC) = 15.7 Hz, C-2], 10.9 [d, ^3J(PC) = 11.5 Hz, C-1].

(1,4-Dioxanyl-2-methyl)phenyl(3-(trimethoxysilyl)propyl)phosphine (1c): $^{31}P\{^1H\}$ NMR (toluene) δ −33.8, −37.10 (2s, diastereomers); $^{13}C\{^1H\}$ NMR ($CDCl_3$) δ 138.3, 138.1 [2 d, ^1J(PC) = 15.1, 15.1 Hz, C-*i*], 132.15, 132.13 [2 d, ^2J(PC) = 19.7, 19.5 Hz, C-*o*], 128.6 (C-*p*), 128.2 [d, ^3J(PC) = 7.1 Hz, C-*m*], 73.8, 73.3 [2 d, ^2J(PC) = 14.2, 16.5 Hz, C-6], 71.8, 71.6 [2 d, ^3J(PC) = 8.8, 10.1 Hz, C-11], 66.6 (C-8), 66.0 (C-9), 50.0 ($SiOCH_3$), 32.6–31.5 (m, C-5), 31.0–30.4 (m, C-3), 19.1 [d, ^2J(PC) = 16.7 Hz, C-2], 10.7 [d, ^3J(PC) = 11.5 Hz, C-1].

Preparation of the T-Functionalized Ether–Phosphine Ruthenium Complexes 3a–c. $HRuCl(CO)(PPh_3)_3$ (**2**) was refluxed with 3 equiv of **1a–c** in toluene. After evaporation of the solvent under vacuum, the slightly yellow oils were dissolved in *n*-hexane (200 mL) at 60 °C and the solutions allowed to stand overnight at −50 °C to separate the products. The procedure was repeated to remove PPh_3.

Carbonylchlorohydridotris[(2-methoxyethyl)phenyl(3-(trimethoxysilyl)propyl)phosphine-*P*,*P*′,*P*″]ruthenium(II) (3a). A suspension of **1a** (2.253 g, 6.82 mmol) and **2** (2.162 g, 2.27 mmol) in toluene (20 mL) was refluxed for 15 min and treated with *n*-hexane to form a colorless resin (3a, 1.95 g, 74%): ^1H NMR (C_6D_6) δ −7.15 [dt, ^2J(PH) = 110, ^2J(PH) = 26 Hz, RuH]; $^{13}C\{^1H\}$ NMR (C_6D_6) δ 203.7 [q, ^2J(PC) = 13.9 Hz, RuCO], 139.5–126.8 (C-*i*,*o*,*m*,*p*), 69.3–68.7 (C-6), 58.2 (C-8), 50.3 ($SiOCH_3$), 35.5–24.4 (C-3,5), 18.2 (C-2), 11.5 (C-1); $^{31}P\{^1H\}$ NMR (toluene) δ 18.1–14.1 (8d, ^2J(PP) = 18.3 Hz, P^2), −1.0 to −2.2 (m, P^1); ^{31}P MAS NMR (SPE) δ 17.4 (P^2), −1.3 (P^1); ^{29}Si MAS NMR (SPE) δ −42.5; IR (film on NaCl) 3053, 2940, 2893, ν(CO) 1911, 1435, 1190, 1087, 824, 744, 696, 501 cm^{-1}; mass spectrum *m*/*z* 1157 (M^+, 19), 827 (M^+ − **1a**, 100), 791 (M^+ − Cl − **1a**, 44), 330 (**1a**, 78). Elemental Anal. Calcd for $C_{46}H_{82}ClO_{13}P_3RuSi_3$: C, 47.76; H, 7.14; Cl, 3.06; Ru, 8.74. Found: C, 48.28; H, 7.23; Cl, 3.38; Ru, 8.60.

Carbonylchlorohydridotris[(phenyl(tetrahydrofuranyl-2-methyl)(3-(trimethyloxysilyl)propyl)phosphine-*P*,*P*′,*P*″]ruthenium(II) (3b). A suspension of **1b** (2.260 g, 6.34 mmol) and **2** (2.013 g, 2.11 mmol) in toluene (20 mL) was refluxed for 15 min and treated with *n*-hexane to form a

---

(39) Lindner, E.; Bader, A.; Glaser, E.; Pfleiderer, B.; Schumann, W.; Bayer, E. *J. Organomet. Chem.* **1988**, *355*, 45–53.

slightly red glassy solid (**3b**, 1.83 g, 70%): ^{1}H NMR (C_6D_6) δ −7.29 [dt, ^2J(PH) = 106, ^2J(PH) = 25.9 Hz, RuH]; ^{13}C{^{1}H} NMR (C_6D_6) δ 204.1 (q, RuCO), 136.9–126.8 (C-*i*,*o*,*m*,*p*), 76.3 (m, C-6), 67.5 (s, C-8), 50.3 ($SiOCH_3$), 34.1 (s, C-10), 33.5–27.9 (C-3,5), 25.7 (s, C-9), 18.6 (s, C-2), 11.6 (s, C-1); ^{31}P{^{1}H} NMR (toluene) δ 21.3–15.9 (P^2), 0.6 to −0.9 (P^1); ^{31}P CP-MAS NMR δ 18.2 (P^2), −1.4 (P^1); ^{29}Si CP-MAS NMR δ −42.1; IR (KBr) 3063, 2941, 2878, 2839, ν(CO) 1909, 1436, 1190, 1084, 930, 819, 744, 696, 502 cm^{-1}; mass spectrum *m/z* 1234 (M^+ − H, 18), 877.5 (M^+ − H − **1b**, 100), 843.1 (M^+ − Cl − **1b**, 44), 356 (**1h**, 20). Elemental Anal. Calcd for $C_{52}H_{88}ClO_{13}P_3RuSi_3$: C, 50.57; H, 7.18; Cl, 2.87; Ru, 8.19. Found: C, 50.53; H, 7.44; Cl, 3.06; Ru, 8.16.

Carbonylchlorohydridotris[(1,4-dioxanyl-2-methyl)phenyl(3-(trimethoxysilyl)propyl)phosphine-*P*,*P′*,*P″*]ruthenium(II) (3c). A suspension of **1c** (2.260 g, 6.29 mmol) and **2** (2.69 g, 2.01 mmol) in toluene (20 mL) was refluxed for 15 min and treated with *n*-hexane to form a colorless glassy solid (**3c**, 1.73 g, 67%): ^{13}C{^{1}H} NMR (C_6D_6) δ 203.5 (m, RuCO), 139.2–126.8 (C-*i*,*o*,*m*,*p*), 73.4 (C-11), 72.0 (m, C-6), 66.5 (C-8,9), 50.0 ($SiOCH_3$), 31.0–25.5 (C-3,5), 18.5 (C-2), 11.5 (C-1); ^{31}P{^{1}H} NMR (toluene) δ 22.5–18.6 (P^2), 1.0 to −1.4 (P^1); ^{31}P CP-MAS NMR δ 20.1 (P^2), 0.2 (P^1); ^{29}Si CP-MAS NMR δ −42.3; IR (KBr) 3053, 2946, 2909, 2840, 2839, ν(CO) 1912, 1435, 1120, 1083, 911, 879, 815, 747, 696, 502 cm^{-1}; mass spectrum *m/z* 909 (M^+ − H − **1c**, 10), 874 (M^+ − H − Cl − **1c**, 19), 372 (**1c**, 100). Elemental Anal. Calcd for $C_{52}H_{88}ClO_{16}P_3RuSi_3$: C, 48.68; H, 6.91; Cl, 2.76; Ru, 7.88. Found: C, 48.56; H, 6.98; Cl, 2.62; Ru, 7.69.

A. Sol–Gel Processing and Aging Procedures. Method 1 (Gelification). **1a–c** or **3a–c**, the specified quantity of $Si(OEt)_4$, water, and $(nBu)_2Sn(OAc)_2$ were homogenized with the minimum of MeOH. The mixtures were sealed in a Schlenk tube and stirred at ambient temperature until the solutions became viscous (2 h). Solidification occurred by warming to 60 °C for 4 h. Then the solvent was removed, and the gels were dried at 60 °C for 4 h. Solvent processing was performed by stirring the large, brittle gel particles in *n*-hexane (three 100-mL portions within 12 h), leading to fine powders. After the gels were dried under vacuum (2 h), they were washed with water, acetone, and *n*-hexane (four 30-mL portions). Final aging of the materials was carried out by drying at 60 °C under vacuum for 8 h (densities 0.6–0.8 g/mL).

Method 2a (Precipitation). A solution of **3a–c**, $Si(OEt)_4$, water, and $(nBu)_2Sn(OAc)_2$ in methanol (20 mL) was placed in a sealed Schlenk tube. The mixtures were stirred for 4 h at 60 °C, but no gel transition was observed. Subsequently a saturated solution of NH_4HCO_3 (40 mL) was added dropwise under stirring and fine, voluminous precipitates were formed immediately. Methanol was distilled off, and the gels were stirred for 1 h at 60 °C. The precipitates were isolated by centrifugation and washed with water, acetone, and *n*-hexane (four 30-mL portions). The gels were dried under vacuum at 60 °C (4 h) and solvent processed under stirring in *n*-hexane (three 100-mL portions within 12 h). Final drying at 60 °C under vacuum for 8 h yielded fine, creamy-white powders (densities 0.3–0.4 g/mL).

Method 2b. **3a**,**c** were reacted according to method 2a except that solid $MgSO_4$ was added instead of aqueous NH_4HCO_3 to initiate the gel transition. Excess $MgSO_4$ was removed with a solution of NH_4HCO_3 in water (0.1 M) until no Mg^{2+} ions were detected in the washings (densities 0.3–0.4 g/mL).

Method 3. Silica gel was synthesized from $Si(OEt)_4$ (2.0 g, 9.62 mmol), water (1.73 g, 96.2 mmol), and $(nBu)_2Sn(OAc)_2$ (67 mg, 0.19 mmol) in methanol (5 mL). The mixture was stirred and warmed to 60 °C for 4 h in a sealed Schlenk tube. After gelling had occurred, the precipitate was washed with water, acetone, and *n*-hexane (three 30-mL portions). Final drying at 80 °C for 8 h delivered silica gel without $-CH_3$ or $-OCH_2-$ resonances from unhydrolyzed ethoxy groups in the ^{13}C CP MAS NMR spectrum (silica gel, 0.65 g, 115%).

3c′–silica gel was prepared by the cocondensation of silica gel (0.50 g), **3c** (1.373 g, 1.070 mmol), H_2O (173 mg, 9.63 mmol), and $(nBu)_2Sn(OAc)_2$ (11 mg, 0.03 mmol) in methanol (2 mL) at 60 °C for 4 h. After the gel was dried under vacuum (60 °C, 4 h), it was stirred in *n*-hexane (three 100-mL portions within 12 h), dried, and washed with water (three 10-mL portions). Final drying was carried out at 60 °C under vacuum for 8 h (**3c′–silica gel**, 1.38 g).

B. Materials Characterization. The solid-state NMR spectra were recorded on a Bruker MSL 200 multinuclear spectrometer with a wide-bore magnet (4.7 T) using samples of 200–400 mg in double-bearing rotors of ZrO_2. Magic-angle spinning was routinely performed at 4-kHz spinning rates at 297 K unless otherwise noted. All measurements were carried out under exclusion of molecular oxygen. Frequencies and standards: ^{31}P, 81 MHz ($NH_4H_2PO_4$); ^{13}C, 50.325 MHz [TMS, carbonyl resonance of glycin (δ = 170.09) as the second standard]; ^{29}Si, 39.75 MHz (Q_8M_8).[40] Typically, the proton 90° pulse length for ^{31}P and ^{13}C CP-MAS NMR spectra was 5.0 and 7.5 μs for ^{29}Si. The spectra were recorded using spectral widths of 40 kHz (^{31}P), 20 kHz (^{13}C), and 10 kHz (^{29}Si). The repetition time was 2 s for CP-MAS NMR and 200 s for ^{29}Si MAS NMR spectra with ^{1}H high-power decoupling (SPE). ^{13}C CP-MAS NMR spectra were recorded either with a ^{1}H FLIP-back pulse or by using the TOSS[41] pulse sequence. The cross polarization constants T_{PH}, T_{CH}, and T_{SiH} were determined by variation of the contact time (20–25 suitable experiments). The proton relaxation time in the rotating frame $T_{1\rho H}$ was measured by a direct proton spin lock–τ–CP experiment as described by Schaefer and Stejskal.[27] The obtained $T_{1\rho H}$ values were in good agreement to those obtained by contact time variation and therefore support the accuracy of the T_{PH} and T_{CH} values. Because of the difficulty of maintaining a close Hartmann–Hahn match over the contact time period, the ^{29}Si $T_{1\rho H}$ data recorded by contact time variation differed from those measured by the direct proton spin lock–τ–CP experiment. Meaningful T_{SiH} data were obtained by constraining $T_{1\rho H}$ to the reliable value determined by using the spin lock–τ–CP experiment.[31] The $T_{1\rho H}$ values were obtained by a single-exponential fit of the magnetization decays [except samples **3c′**$(Q^n)_{30}$ and **3c′–silica gel**]. The reproducibility of the $T_{1\rho H}$ data was ±1% (^{31}P), ±3% (^{13}C), ±5% (^{29}Si, large signals of the T^3, Q^3, and Q^4 species), and ±8% (^{29}Si, small signals of T^2 and Q^2 species). The $T_{1\rho H}$ data measured via ^{29}Si were obtained by averaging the $T_{1\rho H}$ values of the T^3, Q^3, and Q^4 species, which differed maximally by ±5%. The $T_{1\rho H}$ data detected via P^1 and P^2 in the polysiloxane-bound complexes showed a discrepancy of maximally ±1.5% and were averaged. T_{1P}, T_{1C}, and T_{1Si} values were obtained using the method developed by Torchia.[42] The multiexponential magnetization decays of T_{1P} and T_{1C} were approximated by a biexponential function. T_{1P} values of repeated measurements differed maximally by ±2% and T_{1C} values by ±5%. The contact times for T_{1P}, T_{1C}, and $T_{1\rho H}$ measurements (^{31}P, ^{13}C) were 2 ms for the ether–phosphine ligands and 1 ms for the ruthenium complexes. Unless noted otherwise, $T_{1\rho H}$ measurements via ^{29}Si were routinely carried out at a contact time of 5 ms. T_{1P} and $T_{1\rho H}$ relaxation measurements at variable temperatures were carried out at a spinning rate of 3.4 kHz two times with the same sample to verify the reversibility and reproducibility of the results. The time difference after each change of temperature was 40–60 min, until the tunings at the probe head and the spinning frequency were constant. All the relaxation time data were obtained by using the Bruker software SIMFIT. For quantification of the silyl species in the polysiloxane-bound complexes, ^{29}Si CP-MAS NMR spectra at contact times of 4, 5, 8, and 10 ms were recorded by accumulating 10 000 fid's at each contact time. Peak deconvolution of the spectra was performed with the Bruker software GLINFIT using Gaussian line shapes. The relative amounts I_0 of each of the T^1, T^2, T^3, and Q^2 species in one sample were calculated by inserting their peak areas of the deconvoluted spectra I(4 ms), I(5 ms), I(8 ms), and I(10 ms), the individual T_{SiH} data, and the common $T_{1\rho H}$ value into eq 2. I_0 data of Q^3 and Q^4 species were calculated in the same way from the peak areas I(8 ms) and I(10 ms); the very small I_0 values of the T^1 species were calculated with the T_{SiH} data of the T^2 species. The I_0 values of the species, calculated at the different contact times, were averaged and compared to a ^{29}Si MAS NMR spectrum (SPE). The results of each sample showed a discrepancy of less than ±10% between both methods (see Table 1), except those of **3c′**$(Q^n)_{30}$. The ether–phosphine ligands **1a′**$(Q^n)_2$–**1c′**$(Q^n)_2$ and **1a′**$(Q^n)_{10}$ were quantified by deconvolution of ^{29}Si MAS NMR spectra (SPE) due to the low $T_{1\rho H}$ values.[25] To obtain sufficient S/N ratios in all ^{29}Si MAS NMR spectra (SPE), 200–500 fid's were accumulated; the line widths of the deconvoluted SPE signals were approximately 10–15% larger than those of the signals recorded with cross polarization. T_{1Si} of the silyl species was determined for **3b′**$(Q^n)_6$ (T^2, 44 s; T^3, 44 s; Q^2, 32 s; Q^3, 36 s; Q^4, 45 s).

The degrees of hydrolysis (Table 2) of the T and Q silicons were estimated from ^{13}C CP-MAS NMR spectra. The peak areas of the signals of the residual $-OCH_3$ and $-OCH_2-$ groups from unhydrolyzed T and Q silicon species were referenced against the peak areas of the signals of carbon C-1 in the ether–phosphines. From the ratio T:Q, as determined by quantitative ^{29}Si solid-state NMR spectroscopy, the degree of hydrolysis was estimated. Scanning electron micrographs (SEM) were recorded on a Zeiss DSM 962 instrument with a tungsten cathode. The samples were sputtered with platinum to form layers of 15–20-nm

---

(40) Lippmaa, E.; Samoson, A. *Bruker Rep.* **1982**, *1*, 6.

(41) Dixon, W. T.; Schaefer, J.; Sefcik, M. D.; Stejskal, E. O.; McKay, R. A. *J. Magn. Reson.* **1982**, *49*, 341–345.

(42) Torchia, A. D. *J. Magn. Reson.* **1978**, *30*, 613–616.

thickness. Surface areas were determined by argon sorption analyses and calculated with the BET equation. Solvent vapor adsorption experiments were performed under argon (1 bar, 22 °C) and analyzed gravimetrically (reproducibility of ±10%). Thermal gravimetric analyses of **3b′**$(Q^n)_6$ were run under nitrogen from 25 to 100 °C on a Netsch instrument. Quantitative H_2O analyses by the Karl Fischer method were carried out three times with 500-mg portions of the catalyst **3b′**$(Q^n)_6$ as previously described.[35] Over 100 successful hydrogenation experiments with different batches of the polysiloxane-bound catalysts (0.1 mmol, with respect to ruthenium) were carried out in 100-mL autoclaves under exclusion of oxygen [argon, 7.2 g (100 mmol) of *n*-butyraldehyde (distilled under argon)]. The reproducibility of the turnover frequency data were ±2% with catalysts from the same batch and ±4% with materials from different batches. The temperature curves of the plots (Figure 9A,B) have been recorded from a thermocouple, which was introduced into the reaction medium. The reaction time in the isothermal experiments (Table 5a) has been calculated from the point when the autoclave has reached the stated temperatures. In the nonisothermal catalytic runs, the reaction time has been determined from the point where the exothermic reaction was initiated until to that point where the pressure remained constant. The analyses were performed quantitatively (standard of 2-hexanone) on a GC 6000 Vega Series 2 (Carlo Erba Instruments) with a fid and a capillary column DB-WAX (60 m, 110 °C, isothermal) (carrier gas, He (50 kPa); integrator, 3393A (Hewlett-Packard)).

C. Materials Synthesis. Preparation of the Polysiloxanes According to Method 1. (2-Methoxyethyl)phenyl(polysiloxanylpropyl)phosphine-$(Q^n)_2$ [1a′$(Q^n)_2$]. **1a** (0.952 g, 2.88 mmol), 2 equiv of $Si(OEt)_4$ (1.200 g, 5.76 mmol), water (0.570 g, 31.68 mmol), and $(nBu)_2Sn(OAc)_2$ (30 mg, 0.086 mmol) in methanol (5.0 mL) was sol–gel processed to give a colorless gel. After solvent processing and aging, a white, solid powder was formed [**1a′**$(Q^n)_2$, 1.19 g, 108%]: ^{29}Si CP-MAS NMR δ (silyl species, T_{SiH} constants) −57.9 (T^2, 0.94 ms), −65.7 (T^2, 1.00 ms), −91.2 (Q^2), −100.3 (Q^3, 1.11 ms), −107.9 (Q^4, 2.77 ms); IR (KBr) 3416, 3050, 2939, 2928, 1435, 1102, 1044, 805, 744, 694 cm^{-1}. Elemental Anal. Calcd for $C_{12}H_{18}O_{6.5}PSi_3$: C, 37.77; H, 4.75. Found: C, 34.72; H, 5.29.

(2-Methoxyethyl)phenyl(polysiloxanylpropyl)phosphine$(Q^n)_{10}$ [1a′-$(Q^n)_{10}$]. **1a** (0.317 g, 0.96 mmol), 10 equiv of $Si(OEt)_4$ (2.00 g, 9.60 mmol), water (0.743 g, 41.28 mmol), and $(nBu)_2Sn(OAc)_2$ (37 mg, 0.106 mmol) in methanol (6.0 mL) was sol–gel processed to give a transparent colorless gel. After solvent processing and aging, a white, solid grit was formed [**1a′**$(Q^n)_{10}$, 0.958 g, 111%]: ^{31}P CP-MAS NMR δ −31.9 ($\nu_{1/2}$ = 837 Hz); ^{13}C CP-MAS NMR (FLIP) δ 209.8 (ssb), 138.5 (C-*i*), 130.2 (C-*o*,*m*,*p*), 70.2 (C-6), 51.0 ($SiOCH_3$), 58.9 (C-8), 26.7 (C-3,5), 17.8 (C-2), 13.5 (C-1); ^{29}Si CP-MAS NMR δ −57.4 (T^2), −65.3 (T^3), −92.4 (Q^2), −101.1 (Q^3), −108.7 (Q^4); IR (KBr) 3430, 2963, 2934, 1437, 1187, 1068, 804, 747, 698 cm^{-1}. Elemental Anal. Calcd for $C_{12}H_{18}O_{22.5}PSi_{11}$: C, 16.72; H, 2.10. Found: C, 15.14; H, 2.98.

Phenyl(tetrahydrofuranyl-2-methyl)(polysiloxanylpropyl)phosphine-$(Q^n)_2$ [1b′$(Q^n)_2$]. **1b** (1.009 g, 2.83 mmol), 2 equiv of $Si(OEt)_4$ (1.179 g, 5.66 mmol), water (0.560 g, 31.13 mmol), and $(nBu)_2Sn(OAc)_2$ (30 mg, 0.085 mmol) in methanol (5.0 mL) was sol–gel processed to give a colorless gel. After solvent processing and aging, a white, solid powder was formed [**1b′**$(Q^n)_2$, 1.22 g, 106%]: ^{13}C CP-MAS NMR (TOSS, 3.3 kHz) δ 139.0 (C-*i*), 132.5 (C-*o*), 129.0 (C-*m*,*p*), 77.5 (C-6), 67.5 (C-8), 59.4 ($SiOCH_2$), 32.9 (C-3,5,10), 26.2 (C-9), 18.0 (C-2), 13.6 (C-1); ^{29}Si CP-MAS NMR δ −57.3 (T^2), −64.8 (T^3), −92.3 (Q^2), −100.4 (Q^3), −107.8 (Q^4); IR (KBr) 3407, 3052, 2954, 2931, 1435, 1042, 936, 800, 744, 695 cm^{-1}. Elemental Anal. Calcd for $C_{14}H_{20}O_{6.5}PSi_3$: C, 41.26; H, 4.95. Found: C, 36.81; H, 5.22.

(1,4-Dioxanyl-2-methyl)phenyl(polysiloxanylpropyl)phosphine$(Q^n)_2$ [1c′-$(Q^n)_2$]. **1c** (0.980 g, 2.63 mmol), 2 equiv of $Si(OEt)_4$ (1.096 g, 5.26 mmol), water (0.521 g, 28.93 mmol), and $(nBu)_2Sn(OAc)_2$ (28 mg, 0.079 mmol) in methanol (5.0 mL) was sol–gel processed to give a colorless gel. After solvent processing and aging, a white, solid powder was formed [**1c′**$(Q^n)_2$, 1.15 g, 103%]: ^{13}C CP-MAS NMR (TOSS, 3.3 kHz) δ 139.6 (C-*i*), 129.6 (C-*o*,*m*,*p*), 71.5 (C-6,11), 66.6 (C-8,9), 59.1 ($SiOCH_2$), 26.4 (C-3,5), 18.0 (C-2), 13.5 (C-1); ^{29}Si CP-MAS NMR δ −57.0 (T^2), −64.9 (T^3), −92.9 (Q^2), −100.5 (Q^3), −107.8 (Q^4); IR (KBr) 3420, 3071, 2959, 2928, 2856, 1436, 1104, 1042, 907, 877, 800, 744, 695 cm^{-1}. Elemental Anal. Calcd for $C_{14}H_{20}O_{7.5}PSi_3$: C, 39.70; H, 4.76. Found: C, 36.48; H, 5.35.

Carbonylchlorohydridotris[(2-methoxyethyl)phenyl(polysiloxanylpropyl)-phosphine-*P*,*P′*,*P″*]ruthenium(II)$(Q^n)_6$[3a′$(Q^n)_6$]. A mixture of **3a** (0.917 g, 0.793 mmol), 6 equiv of $Si(OEt)_4$ (0.992 g, 4.76 mmol), water (0.471 g, 26.18 mmol), and $(nBu)_2Sn(OAc)_2$ (25 mg, 0.071 mmol) in methanol (4.0 mL) was sol–gel processed to give a slightly yellow gel. A solid, creamy-white powder was formed after solvent processing [**3a′**$(Q^n)_6$, 1.14 g, 110%]: ^{29}Si CP-MAS NMR δ −51.2 (T^1), −58.7 (T^2), −64.4 (T^3), −92.3 (Q^2), −100.4 (Q^3), −107.6 (Q^4); IR (KBr) 3403, 3053, 2927, 2890, 2840, ν(CO) 1915, 1435, 1168, 1101, 954, 802, 744, 697, 502, 455 cm^{-1}. Elemental Anal. Calcd for $C_{37}H_{55}ClO_{20.5}P_3RuSi_9$: C, 33.92; H, 4.23; Cl, 2.71; Ru, 7.72. Found: C, 31.37; H, 4.80; Cl, 2.68; Ru, 7.55.

Carbonylchlorohydridotris[phenyl(tetrahydrofuranyl-2-methyl)(polysiloxanylpropyl)phosphine-*P*,*P′*,*P″*]ruthenium(II)$(Q^n)_6$ [3b′$(Q^n)_6$]. A mixture of **3b** (1.938 g, 1.569 mmol), 6 equiv of $Si(OEt)_4$ (1.960 g, 9.41 mmol), water (0.932 g, 51.78 mmol), and $(nBu)_2Sn(OAc)_2$ (50 mg, 0.141 mmol) in methanol (8.0 mL) was sol–gel processed to give a slightly yellow gel. A solid, creamy-white powder was formed after solvent processing [**3b′**$(Q^n)_6$, 2.29 g, 105%]: ^{13}C CP-MAS NMR (TOSS, 3.3 kHz) δ 129.5 (C-*i*,*o*,*m*,*p*), 75.3 (C-6), 67.7 (C-8), 33.3 (C-3,5,10), 26.4 (C-9), 18.0 (C-2), 14.0 (C-1); IR (KBr) 3401, 3052, 2954, ν(CO) 1917, 1434, 1087, 939, 801, 744, 696 cm^{-1}. Elemental Anal. Calcd for $C_{43}H_{61}ClO_{20.5}P_3RuSi_9$: C, 37.20; H, 4.43; Cl, 2.55; Ru, 7.28. Found: C, 34.80; H, 4.86; Cl, 2.42; Ru, 6.72; H_2O, 3.11 (Karl Fischer analysis) and 2.97 (thermal gravimetric analysis). Calcd for $C_{43}H_{61}ClO_{20.5}P_3RuSi_9(O_{0.5}H)_{5.2}(H_2O)_{2.5}$: C, 34.90; H, 4.85; Cl, 2.40; Ru, 6.83; H_2O, 3.04.

Carbonylchlorohydridotris[(1,4-dioxanyl-2-methyl)phenyl(polysiloxanylpropyl)phosphine-*P*,*P′*,*P″*]ruthenium(II)$(Q^n)_6$[3c′$(Q^n)_6$]. A mixture of **3c** (0.827 g, 0.670 mmol), 6 equiv of $Si(OEt)_4$ (0.837 g, 4.02 mmol), water (0.398 g, 22.11 mmol), and $(nBu)_2Sn(OAc)_2$ (21 mg, 0.060 mmol) in methanol (3.5 mL) was sol–gel processed to give a slightly yellow gel. A solid, creamy-white powder was formed after solvent processing [**3c′**-$(Q^n)_6$, 0.991 g, 103%]: ^{13}C CP-MAS NMR (TOSS, 3.3 kHz) δ 129.3 (C-*i*,*o*,*m*,*p*), 71.9 (C-6,11), 66.4 (C-8,9), 58.7 ($SiOCH_2$), 50.4 ($SiOCH_3$), 26.5 (C-3,5), 17.9 (C-2), 13.9 (C-1); ^{29}Si CP-MAS NMR δ −51.7 (T^1), −57.8 (T^2), −65.0 (T^3), −92.7 (Q^2), −101.1 (Q^3), −108.5 (Q^4); IR (KBr) 3409, 2955, 2853, ν(CO) 1920, 1435, 1120, 1101, 911, 879, 808, 743, 696, 455 cm^{-1}. Elemental Anal. Calcd for $C_{43}H_{61}ClO_{23.5}P_3RuSi_9$: C, 35.96; H, 4.28; Cl, 2.47; Ru, 7.04. Found: C, 35.74; H, 4.89; Cl, 2.32; Ru, 6.99.

Carbonylchlorohydridotris[(1,4-dioxanyl-2-methyl)phenyl(polysiloxanylpropyl)phosphine-*P*,*P′*,*P″*]ruthenium(II)$(Q^n)_{10}$[3c′$(Q^n)_{10}$]. A mixture of **3c** (0.405 g, 0.316 mmol), 10 equiv of $Si(OEt)_4$ (0.658 g, 3.16 mmol), water (0.279 g, 15.48 mmol), and $(nBu)_2Sn(OAc)_2$ (14 mg, 0.041 mmol) in methanol (3.0 mL) was reacted to give a slightly yellow gel. A solid, creamy-white powder was formed after solvent processing [**3c′**$(Q^n)_{10}$, 0.577 g, 109%]: ^{31}P CP-MAS NMR δ 20.1 (P^2), 2.2 (P^1); ^{13}C CP-MAS NMR (TOSS, 3.3 kHz) δ 129.4 (C-*i*,*o*,*m*,*p*), 71.8 (C-6,11), 66.6 (C-8,9), 58.8 ($SiOCH_2$), 50.5 ($SiOCH_3$), 27.4 (C-3,5), 17.7 (C-2), 14.1 (C-1); ^{29}Si CP-MAS NMR (silyl species, T_{SiH} constants) δ −50.5 (T^1), −57.3 (T^2, 1.26 ms), −65.1 (T^3, 1.46), −92.2 (Q^2, 1.06), −100.2 (Q^3 , 1.66), −108.4 (Q^4, 2.91); IR (KBr) 3409, 3060, 2961, 2929, ν(CO) 1920, 1438, 1067, 909, 878, 791, 744, 695, 428 cm^{-1}. Elemental Anal. Calcd for $C_{43}H_{61}ClO_{31.5}P_3RuSi_{13}$: C, 30.81; H, 3.67; Cl, 2.11; Ru, 6.03. Found: C, 29.57; H, 4.38; Cl, 1.87; Ru, 5.83.

Carbonylchlorohydridotris[(1,4-dioxanyl-2-methyl)phenyl(polysiloxanylpropyl)phosphine-*P*,*P′*,*P″*]ruthenium(II)$(Q^n)_{30}$[3c′$(Q^n)_{30}$]. A mixture of **3c** (0.371 g, 0.289 mmol), 30 equiv of $Si(OEt)_4$ (1.806 g, 8.67 mmol), water (0.671 g, 37.28 mmol), and $(nBu)_2Sn(OAc)_2$ (33 mg, 0.095 mmol) in methanol (6.0 mL) was sol–gel processed to give a slightly yellow gel. A solid, creamy-white powder was formed after solvent processing [**3c′**-$(Q^n)_{30}$, 0.910 g, 109%]: ^{31}P CP-MAS NMR δ 20.2 (P^2), 1.7 (P^1); ^{13}C CP-MAS NMR (TOSS, 3.3 kHz) δ 129.6 (C-*i*,*o*,*m*,*p*), 71.2 (C-6,11), 66.5 (C-8,9), 59.7 ($SiOCH_2$), 26.7 (C-3,5), 17.4 (C-2), 13.7 (C-1); ^{29}Si CP-MAS NMR (silyl species, T_{SiH} constants) δ −51.6 (T^1), −58.4 (T^2, 1.10 ms), −64.4 (T^3, 1.22 ms), −91.7 (Q^2, 1.03 ms), −101.6 (Q^3, 1.42 ms), −109.1 (Q^4, 3.14 ms); IR (KBr) 3419, 2964, 2910, ν(CO) 1920, 1439, 1058, 795, 747, 695, 454 cm^{-1}. Elemental Anal. Calcd for $C_{43}H_{61}ClO_{71.5}P_3RuSi_{33}$: C, 17.94; H, 3.67; Cl, 1.23; Ru, 3.51. Found: C, 16.24; H, 3.18; Cl, 0.99; Ru, 3.43.

Preparation of Polysiloxane-Bound Complexes According to Method 2a. Carbonylchlorohydridotris[(2-methoxyethyl)phenyl(polysiloxanylpropyl)phosphine-*P*,*P′*,*P″*]ruthenium(II)$(Q^n)_{3.4}$ [3a′$(Q^n)_{3.4}$]. A solution of **3a** (1.052 g, 0.909 mmol), 6 equiv of $Si(OEt)_4$ (1.136 g, 5.45 mmol), water (0.540 g, 29.98 mmol), and $(nBu)_2Sn(OAc)_2$ (29 mg, 0.082 mmol) was stirred in methanol (20.0 mL) and treated with NH_4HCO_3/H_2O (40 mL). Fine, creamy-white powder [**3a′**$(Q^n)_{3.4}$, 1.10 g, 92%]: ^{31}P CP-MAS NMR δ 17.6 (P^2), −1.2 (P^1); ^{13}C CP-MAS NMR (TOSS, 3.3 kHz) δ 129.6 (C-*i*,*o*,*m*,*p*), 67.5 (C-6), 58.7 (C-8), 50.0 ($SiOCH_3$), 27.0 (C-3,5), 18.0 (C-2), 14.6 (C-1); ^{29}Si CP-MAS NMR δ −50.6 (T^1), −58.4 (T^2), −66.3 (T^3), −92.4 (Q^2), −100.5 (Q^3), −109.1 (Q^4); IR (KBr) 3389, 3055, 2928, ν(CO) 1918, 1435, 1103, 954, 804, 744, 697, 488 cm^{-1}. Elemental Anal. Calcd for $C_{37}H_{55}ClO_{15.3}P_3RuSi_{6.4}$: C, 38.51; H, 4.80; Cl, 3.07; Ru, 8.76. Found: C, 39.03; H, 5.09; Cl, 2.89; Ru, 8.47.

Carbonylchlorohydridotris[phenyl(tetrahydrofuranyl-2-methyl)(polysiloxanylpropyl)phosphine-*P,P′,P″*]ruthenium(II)$(Q^n)_{4.4}$ [3b′$(Q^n)_{4.4}$]. A solution of **3b** (1.142 g, 0.925 mmol), 6 equiv of $Si(OEt)_4$ (1.156 g, 5.55 mmol), water (0.550 g, 30.53 mmol), and $(n\mathrm{Bu})_2Sn(OAc)_2$ (29 mg, 0.083 mmol) was stirred in methanol (20.0 mL) and treated with NH_4HCO_3/H_2O (40 mL). Fine, creamy-white powder [**3b′**$(Q^n)_{4.4}$, 1.21 g, 94%]: ^{31}P CP-MAS NMR δ 18.5 (P^2), –1.3 (P^1); ^{13}C CP-MAS NMR (TOSS, 3.3 kHz) δ 128.7 (C-*i,o,m,p*), 76.2 (C-6), 67.4 (C-8), 32.4 (C-3,5,10), 26.4 (C-9), 17.9 (C-2), 14.1 (C-1); ^{29}Si CP-MAS NMR δ –50.1 (T^1), –58.9 (T^2), –67.4 (T^3), –92.7 (Q^2), –100.8 (Q^3), –109.0 (Q^4); IR (KBr) 3408, 3053, 2954, ν(CO) 1919, 1435, 1090, 939, 798, 744, 696, 448 cm^{-1}. Elemental Anal. Calcd for $C_{43}H_{61}ClO_{17.3}P_3RuSi_{7.4}$: C, 39.97; H, 4.76; Cl, 2.74; Ru, 7.83. Found: C, 37.27; H, 4.83; Cl, 2.58; Ru, 7.82.

Carbonylchlorohydridotris[(1,4-dioxanyl-2-methyl)phenyl(polysiloxanylpropyl)phosphine-*P,P′,P″*]ruthenium(II)$(Q^n)_{4.2}$ [3c′$(Q^n)_{4.2}$]. A solution of **3c** (1.089 g, 0.849 mmol), 6 equiv of $Si(OEt)_4$ (1.061 g, 5.09 mmol), water (0.504 g, 28.00 mmol), and $(n\mathrm{Bu})_2Sn(OAc)_2$ (27 mg, 0.076 mmol) was stirred in methanol (20.0 mL) and treated with NH_4HCO_3/H_2O (40 mL). Fine, creamy-white powder [**3c′**$(Q^n)_{4.2}$, 1.17 g, 96%]: ^{31}P CP-MAS NMR δ 21.0 (P^2), 2.1 (P^1); ^{13}C CP-MAS NMR (TOSS, 3.3 kHz) δ 129.6 (C-*i,o,m,p*), 72.0 (C-6,11), 66.4 (C-8,9), 50.7 ($SiOCH_3$), 26.8 (C-3,5), 18.2 (C-2), 13.9 (C-1); ^{29}Si CP-MAS NMR (silyl species, T_{SiH} constants) δ –49.9 (T^1, 0.69 ms), –58.5 (T^2, 1.03 ms), –64.6 (T^3, 1.20 ms), –92.0 (Q^2, 0.81 ms), –101.1 (Q^3, 1.47 ms), –108.5 (Q^4, 2.64 ms); IR (K Br) 3416, 3052, 2957, 2925, 2853, ν(CO) 1919, 1435, 1120, 1101, 911, 879, 798, 744, 697, 456 cm^{-1}. Elemental Anal. Calcd for $C_{43}H_{61}ClO_{19.9}P_3RuSi_{7.2}$: C, 38.89; H, 4.63; Cl, 2.67; Ru, 7.61. Found: C, 37.70; H, 5.32; Cl, 2.19; Ru, 7.11.

Preparation of the Polysiloxanes According to Method 2b. Mg^{2+}-Doped Carbonylchlorohydridotris[(2-methoxyethyl)phenyl(polysiloxanylpropyl)phosphine-*P,P′,P″*]ruthenium(II)$(Q^n)_3$ [3a′$(Q^n)_3$]. A solution of **3a** (1.114 g, 0.963 mmol), 3 equiv of $Si(OEt)_4$ (0.602 g, 2.89 mmol), water (0.572 g, 20.23 mmol), and $(n\mathrm{Bu})_2Sn(OAc)_2$ (20 mg, 0.058 mmol) was stirred in methanol (20.0 mL) and treated with solid $MgSO_4$ (2.00 g, 16.61 mmol) to give a creamy-white powder [**3a′**$(Q^n)_3$, 1.20 g, 110%]: ^{31}P CP-MAS NMR δ 17.0 (P^2), –1.9 (P^1); ^{13}C CP-MAS NMR (TOSS, 3.3 kHz) δ 138.2 (C-*i*), 129.4 (C-*o,m,p*), 69.3 (C-6), 58.9 (C-8), 51.1 ($SiOCH_3$), 26.8 (C-3,5), 17.9 (C-2), 14.1 (C-1); ^{29}Si CP-MAS NMR δ –51.7 (T^1), –59.8 (T^2), –65.6 (T^3), –86.8 ($Q^{2\prime}$), –92.7 (Q^2), –100.4 (Q^3), –107.2 (Q^4); IR (KBr) 3412, 3054, 2928, ν(CO) 1914, 1434, 1160, 1100, 954, 808, 744, 697, 502, 445 cm^{-1}. Elemental Anal. Calcd for $C_{37}H_{55}ClO_{13.5}P_3RuSi_6Mg_{0.20}$: C, 39.16; H, 4.89; Cl, 3.12; Ru, 8.91; Mg, 0.43. Found: C, 36.43; H, 5.39; Cl, 2.67; Ru, 7.54; Mg, 0.43. Hydrogenations of *n*-butyraldehyde (100–130 °C, Ru:*n*-butyraldehyde = 1:1000, reaction time of 6–7 min for quantitative conversion into *n*-butanol in catalytic runs 1–3) were as follows. Catalytic run 1: IR (KBr) ν(CO) 1916, 1964, 2044 cm^{-1}. Elemental Anal. Found: C, 37.08; H, 5.24; Cl, 2.82; Ru, 7.6. Catalytic run 2: IR (KBr) ν(CO) 1916, 1963, 2044 cm^{-1}. Elemental Anal. Found: C, 36.54; H, 5.00; Cl, 3.12; Ru, 7.5. Catalytic run 3: IR (KBr) ν(CO) 1917, 1961, 2044 cm^{-1}. Elemental Anal. Found: C, 36.45; H, 5.05; Cl, 2.94; Ru, 7.58.

Mg^{2+}-Doped Carbonylchlorohydridotris[(1,4-dioxanyl-2-methyl)phenyl(polysiloxanylpropyl)phosphine-*P,P′,P″*]ruthenium(II)$(Q^n)_6$[3c′$(Q^n)_6$]. A solution of **3c** (1.089 g, 0.849 mmol), 6 equiv of $Si(OEt)_4$ (1.061 g, 5.09 mmol), water (0.504 g, 28.00 mmol), and $(n\mathrm{Bu})_2Sn(OAc)_2$ (27 mg, 0.076 mmol) was stirred in methanol (20.0 mL) and treated with solid $MgSO_4$ (2.00 g, 16.61 mmol) to give a creamy-white powder [**3c′**$(Q^n)_6$, 1.38 g, 112%]: ^{31}P CP-MAS NMR δ 20.1 (P^2), 1.9 (P^1); ^{13}C CP-MAS NMR (TOSS, 3.3 kHz) δ 129.5 (C-*i,o,m,p*), 71.2 (C-6,11), 66.4 (C-8,9), 49.9 ($SiOCH_3$), 26.6 (C-3,5), 18.0 (C-2), 14.0 (C-1); ^{29}Si CP-MAS NMR (silyl species, T_{SiH} constants) δ –50.5 (T^1, 0.80 ms), –57.9 (T^2, 0.98 ms), –66.7 (T^3, 1.21 ms), –81.0 ($Q^{1\prime}$), –86.5 ($Q^{2\prime}$, 1.05 ms), –92.5 (Q^2, 1.08 ms), –101.0 (Q^3, 2.12 ms), –109.1 (Q^4, 4.08 ms); IR (KBr) 3410, 3056, 2955, 2848, ν(CO) 1919, 1120, 1100, 911, 879, 814, 744, 697, 458 cm^{-1}. Elemental Anal. Calcd for $C_{43}H_{61}ClO_{23.5}P_3RuSi_9Mg_{0.62}$: C, 35.59; H, 4.24; Cl, 2.44; Ru, 6.97; Mg, 1.03. Found: C, 32.50; H, 4.51; Cl, 2.07; Ru, 5.95; Mg, 1.04.

Experimental Data of Samples Prepared According to Method 3. Silica Gel: Surface area, 180 m^2/g; particle size distribution, 10–30 μm; porous surface (SEM); ^{13}C CP-MAS NMR (FLIP) δ 26.7–13.1 [weak resonances from $Sn(CH_2)_3CH_3$]; ^{29}Si CP-MAS NMR δ –91.5 (Q^2), –101.1 (Q^3), –109.9 (Q^4); IR (KBr) 3449, 2962, 1176, 804, 456 cm^{-1}.

Carbonylchlorohydridotris[(1,4-dioxanyl-2-methyl)phenyl(polysiloxanylpropyl)phosphine-*P,P′,P″*]ruthenium(II)–silica gel (3c′–silica gel): ^{31}P CP-MAS NMR δ 20.6 (P^2), 1.9 (P^1); ^{13}C CP-MAS NMR (TOSS, 3.3 kHz) δ 128.7 (C-*i,o,m,p*), 71.5 (C-6,11), 66.1 (C-8,9), 50.1 ($SiOCH_3$), 26.2 (C-3,5), 18.0 (C-2), 13.7 (C-1); ^{29}Si CP-MAS NMR δ –43.4 (T^0), –50.8 (T^1), –57.4 (T^2), –66.8 (T^3), –92.7 (Q^2), –101.6 (Q^3), –109.8 (Q^4); IR (KBr) 3419, 3059, 2957, 2854, ν(CO) 1918, 1436, 1119, 1100, 910, 879, 805, 744, 696 cm^{-1}. Elemental Anal. Found: C, 35.46; H, 4.90; Cl, 2.37; Ru, 7.01.

Acknowledgment. The support of this research by the Deutsche Forschungsgemeinschaft, Bonn/Bad Godesberg, by the Fonds der Chemischen Industrie, Frankfurt/Main, and by the Land Baden Württemberg (Forschungsschwerpunkt) is gratefully acknowledged. We owe thanks to E. Nadler and Prof. W. Göpel, Institut für Physikalische und Theoretische Chemie, University of Tübingen, for SEM micrographs and Dr. K. P. Shdanova and Dr. K. E. Chwa, Institute for Oil-Carbon Synthesis, University of Irkutsk, for argon sorption analyses. We are also grateful to Dr. A. Bader and Dr. K. Eichele for helpful discussions and Dr. K. Albert, Institut für Organische Chemie, University of Tübingen, for valuable cooperation.

Supplementary Material Available: Plots of intensities as functions of the contact time [**3b′**$(Q^n)_6$ (^{29}Si), **1a′**$(Q^n)_2$, and **3a′**$(Q^n)_6$ (^{31}P)], tables of ^{31}P relaxation time data and line widths from Figure 4A–E as functions of the temperature, schematic description of the autoclaves used for the hydrogenation experiments, and selected SEM micrographs of materials prepared according to methods 1–3 (6 pages). This material is contained in many libraries on microfiche, immediately follows this article in the microfilm version of the journal, and can be ordered from the ACS; see any current masthead page for ordering information.